AFRL-AFOSR-UK-TR-2017-0007

Boundary-layer bypass transition over large-scale bodies

Pierre Ricco
UNIVERSITY OF SHEFFIELD, DEPARTMENT OF PSYCHOLOGY

12/16/2016
Final Report

Air Force Research Laboratory
AF Office Of Scientific Research (AFOSR)/ IOE
Arlington, Virginia 22203
Air Force Materiel Command

REPORT DOCUMENTATION PAGE

Form Approved
OMB No. 0704-0188

1. REPORT DATE *(DD-MM-YYYY)*	**2. REPORT TYPE**	**3. DATES COVERED** *(From - To)*
11-02-2017	Final	01 Sep 2013 to 31 Aug 2016

4. TITLE AND SUBTITLE
Boundary-layer bypass transition over large-scale bodies

5a. CONTRACT NUMBER

5b. GRANT NUMBER
FA8655-13-1-3073

5c. PROGRAM ELEMENT NUMBER
61102F

6. AUTHOR(S)
Pierre Ricco

5d. PROJECT NUMBER

5e. TASK NUMBER

5f. WORK UNIT NUMBER

7. PERFORMING ORGANIZATION NAME(S) AND ADDRESS(ES)
UNIVERSITY OF SHEFFIELD, DEPARTMENT OF PSYCHOLOGY
FIRTH CT
SHEFFIELD, S10 2TP GB

8. PERFORMING ORGANIZATION REPORT NUMBER

9. SPONSORING/MONITORING AGENCY NAME(S) AND ADDRESS(ES)
EOARD
Unit 4515
APO AE 09421-4515

10. SPONSOR/MONITOR'S ACRONYM(S)
AFRL/AFOSR IOE

11. SPONSOR/MONITOR'S REPORT NUMBER(S)
AFRL-AFOSR-UK-TR-2017-0007

12. DISTRIBUTION/AVAILABILITY STATEMENT
A DISTRIBUTION UNLIMITED: PB Public Release

13. SUPPLEMENTARY NOTES

14. ABSTRACT
The results suggest that the mean pressure gradient modifies the shape of the streamwise velocity profile compared to the flat-plate boundary layer. The research showed that the streamwise wavenumber plays a key role in the development of the streaks.

15. SUBJECT TERMS
EOARD, BOUNDARY-LAYER, BYPASS TRANSITION

16. SECURITY CLASSIFICATION OF:			**17. LIMITATION OF ABSTRACT**	**18. NUMBER OF PAGES**	**19a. NAME OF RESPONSIBLE PERSON**
a. REPORT	**b. ABSTRACT**	**c. THIS PAGE**			CUMMINGS, RUSSELL
Unclassified	Unclassified	Unclassified	SAR	44	**19b. TELEPHONE NUMBER** *(Include area code)* 011-44-1895-616021

Standard Form 298 (Rev. 8/98)
Prescribed by ANSI Std. Z39.18

Boundary-layer bypass transition over large scale bodies

Grant number: FA8655-13-1-3073 DEF

Principal investigator: Pierre Ricco

Ph.D. student: Eva Zincone

Period of performance:1 September 2013 - 30 November 2016

Department of Mechanical Engineering

University of Sheffield

December 19, 2016

CONTENTS

1. Summary 5

2. Introduction 6
2.1 Objectives 8

3. Methods, assumptions and procedures 9
3.1 Mathematical formulation of the flow around a Rankine body 9
3.1.1 Scaling and change of coordinates 9
3.1.2 The mean flow 12
3.1.3 The perturbation flow 16
3.1.4 Inner perturbation flow 21

4. Results and discussion 24
4.1 Mean flow solution 24
4.1.1 Mean pressure 24
4.1.2 Boundary layer thickness 24
4.1.3 Inner mean velocity 26
4.2 Outer flow solution 26
4.3 Boundary region solution 29

5. Conclusions 30
5.1 Future work 30

Future work 30

Appendix 31

A. Derivation of continuity and Navier-Stokes equations in optimal coordinates . . . 32

B. Numerical procedure for boundary layer equations 38

Bibliography 40

Acknowledgements 40

LIST OF FIGURES

3.1 Perturbed flow around the body. The origin of Cartesian and polar coordinate system is in the point source. At the stagnation point a rotate coordinate system is used. The asymptotic regions around the body are shown. 10
3.2 Comparison between the outer mean velocity on the body and the asymptotic solution close to the stagnation point. In the neighbourhood of the stagnation point the behavior is the same. 13
3.3 Outer mean velocity on the body surface as a function of s. 13

4.1 Mean pressure gradient as a function of s along the body. 24
4.2 Composite solution of the mean flow. 26
4.3 Boundary layer thickness as a function of s (top) and inner mean velocity profiles at different positions on the body (bottom). 27
4.4 Outer perturbation potential. 28
4.5 Outer perturbation pressure. 28
4.6 Outer perturbation velocity. 28
4.7 Profile of streamwise perturbation velocity $\bar{u}$ at the indicated values of $\bar{\Phi}$. . 29
4.8 Profile of spanwise perturbation velocity $\bar{w}$ at the indicated values of $\bar{\Phi}$. . . 29
4.9 Profile of streamwise perturbation velocity $\bar{u}$ at the indicated values of κ and $\bar{\Phi} = 0.5$. 29

A.1 Outer potential velocity in x-y plane and Φ-Ψ plane. 33
A.2 Change of coordinates. 34

B.1 Grid used to compute the velocity components and pressure. 38

LIST OF TABLES

3.1 Decomposition of the flow around the Rankine body 11

1. SUMMARY

It is known that friction due to boundary layer disturbances can affect the performances of many engineering systems and there are many works on the suppression of the transitional boundary layer. Most of the results in the literature are for the flat-plate boundary layer but the behaviour of the velocity and pressure changes with the curvature. This work aims to extend the results of the flat-plate boundary layer to a Rankine-body boundary layer.

A small amplitude, unsteady, three-dimensional perturbation of a mean base flow is considered. The flow is taken incompressible and the Reynolds number high. The analysis is performed in a new special coordinate system, where the streamwise coordinate is replaced by the potential function and the wall normal coordinate by the stream function.

The external flow is decomposed into a mean flow and a perturbation flow. The first one is known and it is given by a uniform flow which encounters a source flow because the presence of the body can be seen as a point source. The perturbation flow around and far from the body is solved by applying WKBJ theory, a method to obtain approximated solutions of linear differential equations whose the highest derivative is multiplied by a small parameter.

In the viscous region near the body, the flow is also decomposed into a mean flow and a perturbation flow. The base flow satisfies the steady mean flow equations in optimal coordinates and since it depends on the streamwise coordinate there is no similarity. Boundary region equations in optimal coordinates for the perturbation flow are obtained. The boundary region equations are numerically solved by imposing no-slip conditions at the wall for the three velocity components and appropriate boundary conditions at a large distance from the body. The latter are found by asymptotic matching between the inner and the outer solution. Differently from the flat plate geometry, the outer pressure disturbance has a role on the boundary layer dynamics and the inner perturbation pressure matches the outer one at a large distance from the body. Another important difference from the flat plate case is that there is a pressure gradient in the inner mean flow. Boundary region equations are parabolic in the streamwise coordinate thus a marching procedure along this coordinate will be used in the code. Initial conditions to start the code are derived.

The results suggest that the mean pressure gradient modifies the shape of the streamwise velocity profile compared to the one of the flat-plate boundary layer. It is observed that the streamwise wavenumber plays a key role in the streaks development.

2. INTRODUCTION

The interaction of a fluid in motion with a solid surface affects the performance of mechanical, aeronautical, civil and chemical engineering systems. When an object moves through a fluid, a boundary layer is created on its surface. In this region viscous effects are not negligible. Boundary layer can either be laminar or turbulent. In the first one the fluid flows in parallel and ordered layers while in the second one the flow is chaotic. Generally, the boundary layer changes from laminar to turbulent through a transitional zone. It has been established that turbulent flows exert a much higher wall friction than laminar flows. Since vehicles such as cars and airplanes, for example, consume an enormous amount of energy due to friction, many works have been directed to the suppression of transitional boundary layer disturbances. It is better achieving drag reduction in the still laminar transitional zone rather than in the already developed turbulent one because suppressing small-amplitude laminar disturbances requires less energy. The reduction of drag has a great technological importance because it implies a significant decrease of the enormous amount of energy consumed by airplanes during flight, moreover flight costs and aerodynamic noise could be reduced and number of passenger per flight could be increased. Such outcomes could limit the global warming effect. Despite the process which governs the transition has been widely studied, at present is not fully understood.

The flow within the boundary layer strongly depends on external flow. It is therefore of utmost importance to study the effects of free stream turbulence (FST) on the boundary layer. FST are defined by the turbulence level (Tu), the turbulence length scales and the turbulence spectrum. Experimental works have confirmed that if Tu is low (< 1 %) the transition from laminar to turbulent boundary layer occurs due to the growth of Tollmien-Schilichting (TS) waves; otherwise, if Tu is high ($> 1\%$) the mechanism which determines the transition from laminar to turbulent is called *bypass transition*. During *bypass transition* the flow is laminar and it is characterised by long streamwise perturbations. These streaks are also called *Klebanoff distortions*, because Klebanoff was among the first to observe them. Due to non-parallel flow effects, these low-frequency components of three-dimensional vortical disturbances in the free stream penetrate the boundary layer and they produce significant distortions in the spanwise direction. There is a large number of direct laboratory investigations of the transition process in the presence of Klebanoff fluctuations.

? observed intermittent appearance of wave packet in the boundary layer at moderate levels of free-stream turbulence. Even if he did not understand the origin of Klebanoff modes he performed many experiments which revealed some important characteristic of the wave packets. They appear only when the turbulence level is higher than a threshold, they grow faster than TS waves and they propagate quickly downstream and slowly in the spanwise direction. Downstream the streaky region turbulent spots appear and then turbulent boundary layer fully develops. While TS wave transitions represent idealised

situations, bypass transitions describe real situations for industrial flow systems.

Bypass transition has been largely studied experimentally and all the results showed that FST induced streamwise streaky structures of alternate high and low velocity in the boundary layer. **?** carried out experiments using techniques like *flow visualisation* and *hot-wire anemometry* in order to determine the effects of FST (in the range of 1-6 %) in the boundary layer. They performed the experiments using grids of various sizes to generate the free-stream turbulence on a test plate. They found that the spanwise scale decreased moving downstream, where it approached the boundary layer thickness. Conversely the streamwise scale increased and it became proportional to the boundary layer thickness, going downstream. They also pointed out that the breakdown of the streaky structures was associated with a secondary instability which seemed to lead to turbulence.

Many authors performed direct numerical simulations (DNS) on bypass transition induced by free-stream turbulence (sometimes in complement with laboratory experiments). **?** depicted eddies and interactions during transition induced by free-stream turbulence. Their simulations showed that when low-frequency modes penetrated the boundary layer, they produced lower frequency modes, which were amplified by the shear and they developed into streaks in the streamwise velocity. Streaks were the same of the experimental measurements of Klebanoff. Simulations of **?** were based on Orr-Sommerfeld theory. This choice allowed to use a rectangular domain and since the lower wall extended over all domain, a better algorithm could be used. Results showed that streaks were stable if they remained near the wall; instead if they lifted up, the disturbance rapidly grew and turbulent spots appeared. Then the spots led to turbulent boundary layer. **?** explored the penetration of external vortical disturbances in the boundary layer, by studying Orr-Sommerfeld and Squire modes interaction. The evolution of modes was analysed by DNS and the domain included boundary region zone. The transition process was simulated with two modes: one strongly coupled and one weakly coupled high-frequency mode. Results showed that if one mode penetrated and the other one no, there was transition. In this paper it was confirmed that low frequencies penetrated the boundary layer and they led to Klebanoff modes.

For a long time bypass transition has only been experimentally observed, but it could not be explained theoretically . The optimal-growth theory was first developed by **?**. The objective of the analysis is to find the optimal perturbations, namely the initial velocity profile which produces the biggest amplification of the disturb. In the Orr-Sommerfeld theory the continuous spectra of the Orr-Sommerfeld equations is used to describe the streaks generated by free-stream turbulence.

? analysed the effects of free-stream turbulence on the pretransitional boundary layer in a flat plate. The free-stream flow is decomposed in a mean flow and a purely convected three-dimensional *perturbation flow*. Their results showed that the free-stream streamwise vorticity is responsible for the generation of the streamwise streaks inside the boundary layer. The streaks are initially amplified then they decay downstream.

? generalised the results of **?** to the unsteady case. They studied the instability of unsteady nonlinear streaks due to free-stream disturbances on an incompressible laminar boundary layer. Their attention was focused on long disturbance wavelengths because it is known that they are responsible for the streaks generation. Their results showed that the nonlinearity can inhibit the amplification of streaks, thus it has a stabilising effect and nonlinear interactions have an effect of distortion on the mean flow. These numerical results

are in agreement with the experimental results of **?**.

? focused on the solution of the external flow around a body of generic shape where a small-amplitude, unsteady, viscous motion was imposed on steady potential flow. He derived the equations for the perturbation velocity and then divided the solution for it in two parts: the first one is the homogeneous solution which satisfies the momentum equation without the forcing term (namely without the pressure gradient); the second one is the potential solution, from which the outer pressure is derived. The total perturbation velocity is given by the summation of these two solutions. He first found the homogeneous solution by WKBJ theory and then from the continuity equation he calculated the potential solution. By using this theory he looked for the phase and the amplitude of the perturbation velocity. The equation for the phase in a new coordinate system is found to be the Eikonal equation. He found a complete analytic solution of the perturbation velocity by changing coordinates. **?** supposed that the steady potential flow is not influenced by viscous effects and to study the problem he included viscous effects in rapid distortion theory. He used his results to calculate the flow over a circular cylinder and he showed the numerical results for large Reynolds numbers. In particular he focused on the behaviour of the streamwise perturbation component velocity along the mean flow stagnation streamline. Its absolute value vanishes when the dimensionless wavenumbers along the perpendicular directions go either to zero or infinity. Moreover, plots of the same function versus the streamwise coordinate show that it decreases as the coordinate goes to zero.

? worked on rapid distortion theory, to extend the work of **?**. He considered compressible flows, with no restrictions on the Mach number value with high Reynolds numbers and he started from the linear inhomogeneous wave equation of a potential function associated with the perturbation velocity. He assumed that the upstream disturbance was a small perturbation of the mean flow. He showed that the perturbation velocity consisted of two parts: one was a known function of the imposed upstream distortion and the mean flow, it had zero-divergence and it was decoupled from the fluctuations in pressure; the other one was an irrotational disturbance, given by the gradient of the potential function which was the solution of the wave equation and it was related to pressure fluctuations. In the paper is also remarked that even without distortion of the mean flow, pressure fluctuations could also be produced by boundary conditions on the surface of the obstacle.

The effect of the curvature combined with a favourable pressure gradient on the streaks are unknown.

2.1 Objectives

- Computing the outer flow dynamics, which is crucial to derive boundary conditions for boundary region equations.
- Analyzing the effect of pressure gradient on the pre-transitional Rankine body boundary layer.
- Studying the evolution of Klebanoff modes inside the boundary layer and identifying the streaks with accelerating mean flow.

3. METHODS, ASSUMPTIONS AND PROCEDURES

3.1 Mathematical formulation of the flow around a Rankine body

The flow around a Rankine body is considered. A sketch of the geometry is shown in figure 3.1. A small amplitude, unsteady, three-dimensional perturbation flow is superimposed to a uniform mean flow upstream. The body can be represented by a flow produced by a point source. When the flow encounters the body both the mean and the perturbation flow are distorted. The flow returns parallel downstream, it is assumed incompressible and high Reynolds numbers based on the characteristic length of the body L^* are considered . The domain is divided in two main asymptotic regions: the outer region around the body but distant from it and the inner small viscous boundary layer region alongside the body. The following hypothesis are made:

- $\lambda^* \ll L^*$ where λ^* represents all the three wavelengths of the disturbance. This hypothesis is valid upstream and it will be used during the analysis of the outer perturbation flow.
- The mean flow is steady and two-dimensional therefore periodicity is assumed along z and t.
- The solution is linear, namely $\epsilon/k_\Phi \ll 1$ inside the boundary layer, therefore terms of order ϵ^2 can be neglected in the equations.

Table 3.1 gives an overview of the asymptotic regions around the Rankine body. In the following sections flows in the outer and inner region will be analysed.

3.1.1 Scaling and change of coordinates

In this section the appropriate scaling is developed and the change of coordinate is described. Lengths which are scaled by L^* (the characteristic length of the body) are indicated by the subscript L. Lengths which are scaled by λ_z^* (the spanwise disturbance wavelenght) do not have any subscript. The velocity components are made dimensionless by U_∞^* , pressure by $\rho^* U_\infty^{*2}$ where ρ^* is the constant density and time by L^*/U_∞^*. All the dimensional quantities are marked by the symbol $*$.

The following continuity and Navier-Stokes equations have to be satisfied by the mean flow

$$\nabla \cdot \mathbf{V} = 0, \tag{3.1}$$

$$\frac{\partial \mathbf{V}}{\partial t_{\mathrm{L}}} + \mathbf{V} \cdot \nabla \mathbf{V} = -\nabla p + \frac{1}{R_{\mathrm{L}}} \nabla \cdot (\nabla \mathbf{V}), \tag{3.2}$$

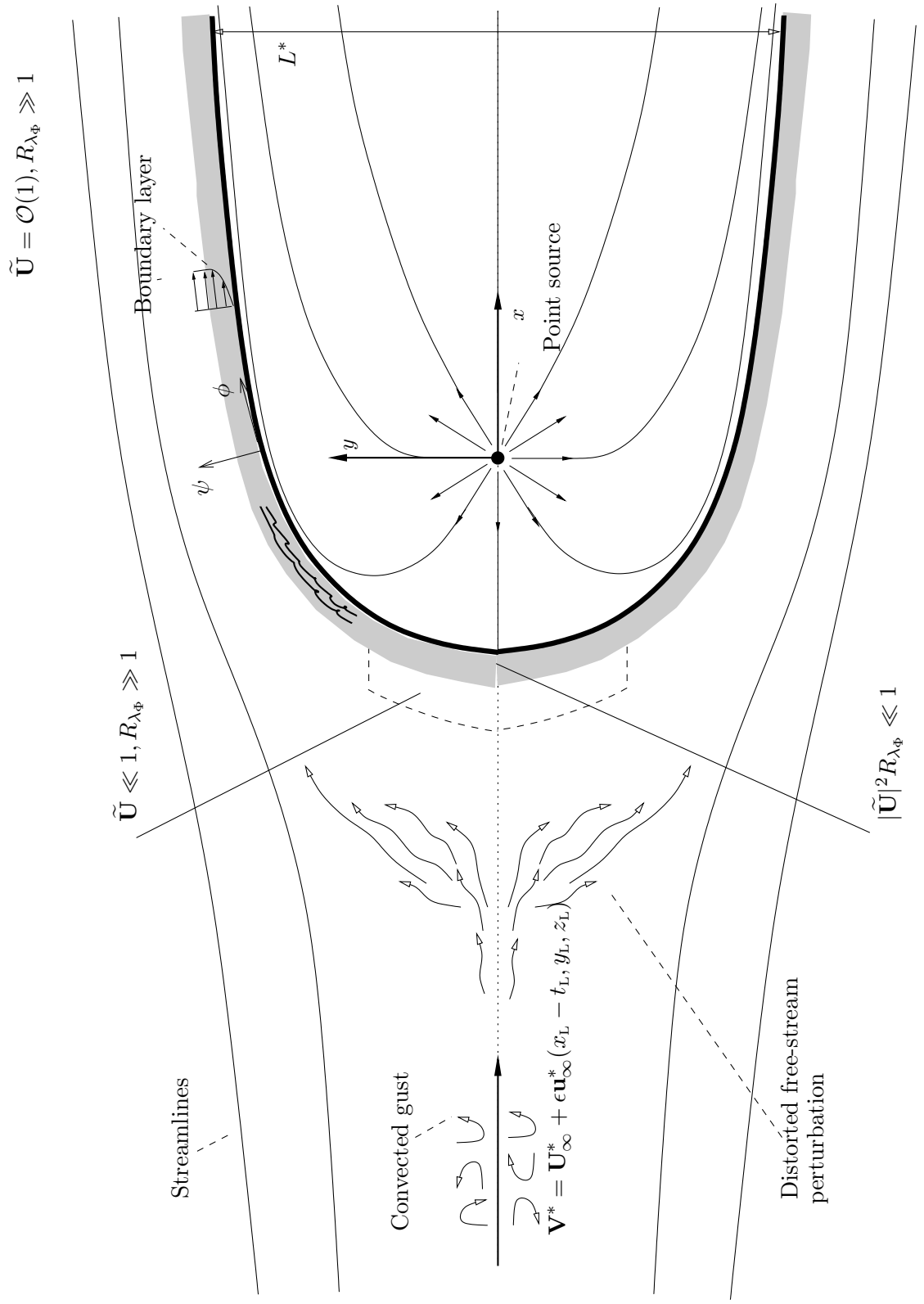

Fig. 3.1: Perturbed flow around the body. The origin of Cartesian and polar coordinate system is in the point source. At the stagnation point a rotate coordinate system is used. The asymptotic regions around the body are shown.

	Mean flow	**Perturbation flow**
Outer	• Inviscid-2D. • Uniform plus source flow. • Pressure gradient. • Stagnation point: Hiemenz flow	• Inviscid-3D. • WKBJ method. • Eikonal equation. • Equation for the amplitude velocity. • Pressure gradient.
Inner	• Viscous-2D. • Steady nonlinear mean flow equation in optimal coordinates.	• Viscous-3D. • Boundary layer equations. • Asymptotic matching with outer flow to obtain boundary conditions. • Derivation of initial conditions.

Tab. 3.1: Decomposition of the flow around the Rankine body

where $R_{\mathrm{L}} = U^*_\infty L^*/\nu^* \gg 1$ is Reynolds number based on L^*, the ∇ operator is in coordinates (x_{L},y_{L},z_{L}) and $\mathbf{V}$ is the vector which represents the total mean flow velocity.

Since the body is not a flat plate, it is convenient to work in a special coordinate system where the streamwise coordinate x_{L} is replaced by the outer mean-flow velocity potential Φ_{L} and the wall normal coordinate y_{L} is replaced by the outer mean-flow stream function Ψ_{L}. In this new coordinate system the geometry is simplified because the streamlines follow the shape of the body, therefore the body is a flat plate in the new system. These coordinates are called optimal coordinates and in Appendix A continuity and Navier-Stokes equations in optimal coordinates are derived. They are

$$\widetilde{U}\frac{\partial w_\Phi}{\partial \Phi_{\mathrm{L}}} + \widetilde{U}\frac{\partial w_\Psi}{\partial \Psi_{\mathrm{L}}} + \frac{\partial w_z}{\partial z_{\mathrm{L}}} = 0, \tag{3.3}$$

$$\frac{1}{\widetilde{U}^2}\frac{\partial w_\Phi}{\partial t_{\mathrm{L}}} + w_\Phi\frac{\partial w_\Phi}{\partial \Phi_{\mathrm{L}}} + w_\Psi\frac{\partial w_\Phi}{\partial \Psi_{\mathrm{L}}} + \frac{1}{\widetilde{U}}w_z\frac{\partial w_\Phi}{\partial z_{\mathrm{L}}} + \frac{\partial \log\widetilde{U}}{\partial \Phi_{\mathrm{L}}}\left(w_\Phi^2 + w_\Psi^2\right) =$$
$$-\frac{1}{\widetilde{U}^2}\frac{\partial p}{\partial \Phi_{\mathrm{L}}} + \frac{1}{R_{\mathrm{L}}}\left[\frac{\partial^2 w_\Phi}{\partial \Phi_{\mathrm{L}}^2} + \frac{\partial^2 w_\Phi}{\partial \Psi_{\mathrm{L}}^2} + \frac{1}{\widetilde{U}^2}\frac{\partial^2 w_\Phi}{\partial z_{\mathrm{L}}^2} - 2\frac{\partial \ln\widetilde{U}}{\partial \Psi_{\mathrm{L}}}\left(\frac{\partial w_\Psi}{\partial \Phi_{\mathrm{L}}} - \frac{\partial w_\Phi}{\partial \Psi_{\mathrm{L}}}\right) - \frac{2}{\widetilde{U}}\frac{\partial \ln\widetilde{U}}{\partial \Phi_{\mathrm{L}}}\frac{\partial w_z}{\partial z_{\mathrm{L}}}\right], \tag{3.4}$$

$$\frac{1}{\widetilde{U}^2}\frac{\partial w_\Psi}{\partial t_{\mathrm{L}}} + w_\Phi\frac{\partial w_\Psi}{\partial \Phi_{\mathrm{L}}} + w_\Psi\frac{\partial w_\Psi}{\partial \Psi_{\mathrm{L}}} + \frac{1}{\widetilde{U}}w_z\frac{\partial w_\Psi}{\partial z_{\mathrm{L}}} + \frac{\partial \log\widetilde{U}}{\partial \Psi_{\mathrm{L}}}\left(w_\Phi^2 + w_\Psi^2\right) =$$
$$-\frac{1}{\widetilde{U}^2}\frac{\partial p}{\partial \Psi_{\mathrm{L}}} + \frac{1}{R_{\mathrm{L}}}\left[\frac{\partial^2 w_\Psi}{\partial \Phi_{\mathrm{L}}^2} + \frac{\partial^2 w_\Psi}{\partial \Psi_{\mathrm{L}}^2} + \frac{1}{\widetilde{U}^2}\frac{\partial^2 w_\Psi}{\partial z_{\mathrm{L}}^2} + 2\frac{\partial \ln\widetilde{U}}{\partial \Phi_{\mathrm{L}}}\left(\frac{\partial w_\Psi}{\partial \Phi_{\mathrm{L}}} - \frac{\partial w_\Phi}{\partial \Psi_{\mathrm{L}}}\right) - \frac{2}{\widetilde{U}}\frac{\partial \ln\widetilde{U}}{\partial \Psi_{\mathrm{L}}}\frac{\partial w_z}{\partial z_{\mathrm{L}}}\right], \tag{3.5}$$

$$\frac{1}{\widetilde{U}^2}\frac{\partial w_z}{\partial t_{\mathrm{L}}} + w_\Phi\frac{\partial w_z}{\partial \Phi_{\mathrm{L}}} + w_\Psi\frac{\partial w_z}{\partial \Psi_{\mathrm{L}}} + \frac{1}{\widetilde{U}}w_z\frac{\partial w_z}{\partial z_{\mathrm{L}}} + w_z\left(w_\Phi\frac{\partial \log\widetilde{U}}{\partial \Phi_{\mathrm{L}}} + w_\Psi\frac{\partial \log\widetilde{U}}{\partial \Psi_{\mathrm{L}}}\right) =$$
$$-\frac{1}{\widetilde{U}^3}\frac{\partial p}{\partial z_{\mathrm{L}}} + \frac{1}{R_{\mathrm{L}}}\left[\frac{\partial^2 w_z}{\partial \Phi_{\mathrm{L}}^2} + \frac{\partial^2 w_z}{\partial \Psi_{\mathrm{L}}^2} + \frac{1}{\widetilde{U}^2}\frac{\partial^2 w_z}{\partial z_{\mathrm{L}}^2} + \frac{w_z}{\widetilde{U}}\left(\frac{\partial^2\widetilde{U}}{\partial \Phi^2} + \frac{\partial^2\widetilde{U}}{\partial \Psi^2}\right) + 2\left(\frac{\partial w_z}{\partial \Phi}\frac{\partial \ln\widetilde{U}}{\partial \Phi_{\mathrm{L}}} + \frac{\partial w_z}{\partial \Psi_{\mathrm{L}}}\frac{\partial \ln\widetilde{U}}{\partial \Psi_{\mathrm{L}}}\right)\right], \tag{3.6}$$

where $\widetilde{U} = |\widetilde{\mathbf{U}}|$ is the amplitude of the outer mean velocity which has its only component along the streamlines, $w_\Phi = u_\Phi/\widetilde{U}$, $w_\Psi = u_\Psi/\widetilde{U}$ and $w_z = w/\widetilde{U}$, with u_Φ and u_Ψ the velocity components in the Φ and Ψ directions respectively.

3.1.2 The mean flow

Outer mean flow

As explained in **?** a combination of uniform flow with a source is well represented in a polar coordinate system,

$$r = \sqrt{x_{\mathrm{L}}^2 + y_{\mathrm{L}}^2}, \qquad \theta = \operatorname{atan}\left(\frac{y_{\mathrm{L}}}{x_{\mathrm{L}}}\right), \tag{3.7}$$

$$\Psi_{\mathrm{L}} = r\sin\theta + \frac{\Lambda\theta}{2\pi} - \frac{\Lambda}{2}, \tag{3.8}$$

$$\Phi_{\mathrm{L}} = r\cos\theta + \frac{\Lambda}{2\pi}\ln r - \frac{\Lambda}{2\pi}\left[\ln\left(\frac{\Lambda}{2\pi}\right) - 1\right], \tag{3.9}$$

where $\Phi_{\mathrm{L}} = \Phi^*/(U_\infty^* L^*)$ is the potential function, $\Psi_{\mathrm{L}} = \Psi^*/(U_\infty^* L*)$ is the stream function and Λ is the dimensionless strength of the source.

The absolute value of the mean outer velocity can be analytically found as a function of r and θ.

$$\widetilde{U} = \sqrt{1 + \frac{\Lambda\cos\theta}{\pi r} + \frac{\Lambda^2}{4\pi^2 r^2}}, \tag{3.10}$$

and therefore the potential, stream function and the mean velocity are known as functions of r and θ. It is not possible to analytically invert the relationships between r-θ and Φ-Ψ, thus this is numerically performed by using Newton-Raphson algorithm.

The expression of r as function of θ and Ψ_{L} is

$$r = \frac{1}{\sin\theta}\left[\Psi_{\mathrm{L}} - \frac{\Lambda\theta}{2\pi} + \frac{\Lambda}{2}\right].$$

The asymptotic behavior of the inner mean flow near the stagnation point in optimal coordinates along the body (streamline equal to zero) has been found by **?** and it is

$$u_{\mathrm{H}} = \sqrt{\frac{4\pi}{\Lambda}\Phi_{\mathrm{L}}}. \tag{3.11}$$

Figure 3.2 shows that in the neighbourhood of the stagnation point the asymptotic solution and the mean velocity overlap. Figure 3.3 shows the outer mean velocity on the body surface $\widetilde{U}_b$ as a function of the coordinate s, which is the coordinate along the body, defined as

$$s = \int \sqrt{1 + \frac{\mathrm{d}y_{\mathrm{L}}}{\mathrm{d}x_{\mathrm{L}}}}\mathrm{d}x_{\mathrm{L}}.$$

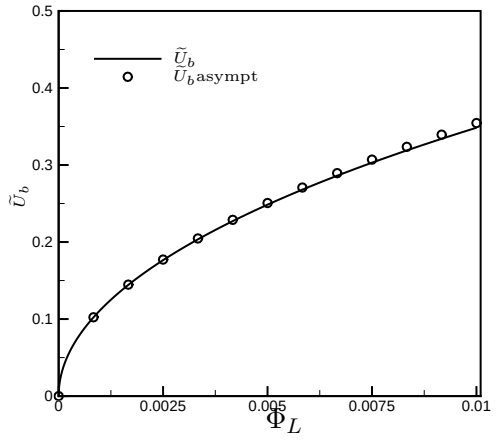

Fig. 3.2: Comparison between the outer mean velocity on the body and the asymptotic solution close to the stagnation point. In the neighbourhood of the stagnation point the behavior is the same.

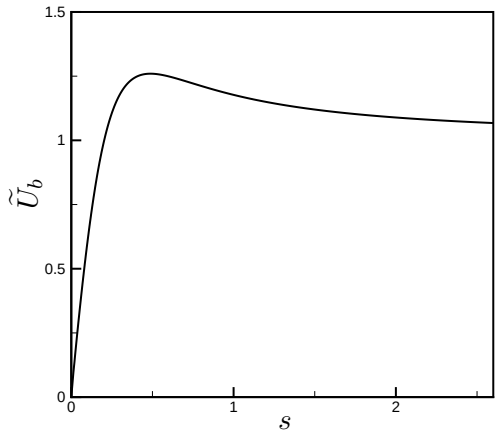

Fig. 3.3: Outer mean velocity on the body surface as a function of s.

Inner mean flow

The continuity and Navier-Stokes equations in the viscous boundary layer in optimal coordinates are obtained by the asymptotic analysis with $R_{\mathrm{L}} \gg 1$. They are

$$\frac{\partial U}{\partial \Phi_{\mathrm{L}}} + \frac{\partial V}{\partial \Psi_{\mathrm{L}}} = 0. \tag{3.12}$$

$$U\frac{\partial U}{\partial \Phi_{\mathrm{L}}}+V\frac{\partial U}{\partial \Psi_{\mathrm{L}}}+\frac{1}{\widetilde{U}_b}\frac{\partial \widetilde{U}_b}{\partial \Phi_{\mathrm{L}}}U^2=-\frac{1}{\widetilde{U}_b^2}\frac{\partial P}{\partial \Phi_{\mathrm{L}}}+\frac{1}{R_{\mathrm{L}}}\frac{\partial^2 U}{\partial \Psi_{\mathrm{L}}^2}, \tag{3.13}$$

$$\frac{\partial P}{\partial \Psi_{\mathrm{L}}}=0, \tag{3.14}$$

Here U and V are the velocity components of the inner mean flow.
Since the inner mean flow is two-dimensional, a stream function can be defined:

$$\bar{\Psi}=F(\Phi_{\mathrm{L}},\eta)\sqrt{\frac{2\Phi_{\mathrm{L}}}{R_{\mathrm{L}}}}, \tag{3.15}$$

where η is the inner variable

$$\eta=\Psi_{\mathrm{L}}\sqrt{\frac{R_{\mathrm{L}}}{2\Phi_{\mathrm{L}}}}, \tag{3.16}$$

By definition

$$U=\frac{\partial \bar{\Psi}}{\partial \Psi_{\mathrm{L}}}=F', \tag{3.17}$$

$$V=-\frac{\partial \bar{\Psi}}{\partial \Phi_{\mathrm{L}}}=-\left[\sqrt{\frac{2\Phi_{\mathrm{L}}}{R_{\mathrm{L}}}}\left(F_{\Phi_{\mathrm{L}}}-F'\frac{\eta}{2\Phi_{\mathrm{L}}}\right)+\frac{F}{2}\sqrt{\frac{2}{R_{\mathrm{L}}\Phi_{\mathrm{L}}}}\right]. \tag{3.18}$$

By substituting (3.17) and (3.18) in (3.13) and using the Bernoulli equation

$$\frac{\mathrm{d}P}{\mathrm{d}\Phi_{\mathrm{L}}}=-\widetilde{U}_b\frac{\mathrm{d}\widetilde{U}_b}{\mathrm{d}\Phi_{\mathrm{L}}},$$

it is obtained:

$$F'''+FF''+2m(\Phi_{\mathrm{L}})[1-F'^2]=2\Phi_{\mathrm{L}}(F'F'_{\Phi_{\mathrm{L}}}-F_{\Phi_{\mathrm{L}}}F''), \tag{3.19}$$

where

$$F'=\frac{\partial F}{\partial \eta},\qquad F_{\Phi}=\frac{\partial F}{\partial \Phi_{\mathrm{L}}},\qquad m=\frac{\Phi_{\mathrm{L}}}{\widetilde{U}_b}\frac{\mathrm{d}\widetilde{U}_b}{\mathrm{d}\Phi_{\mathrm{L}}}.$$

Equations (3.12)-(3.14) have to satisfy the following boundary conditions:

$$U(\Phi_{\mathrm{L}},0)=0,\qquad V(\Phi_{\mathrm{L}},0)=0,\qquad U(\Phi_{\mathrm{L}},\infty)=1, \tag{3.20}$$

which are the no-slip condition at the wall for the two velocity components and the outer boundary condition which states that the velocity must be equal to the outer velocity. The boundary conditions for equation (3.19) are then:

$$F(\Phi_{\mathrm{L}},0)=0,\qquad F'(\Phi_{\mathrm{L}},0)=0,\qquad F'(\Phi_{\mathrm{L}},\infty)=1, \tag{3.21}$$

Equation (3.19) is the most general steady mean flow equation, in optimal coordinates and the flow depends on Φ_{L} therefore it is not similar. It is numerically solved by following

the algorithm in **?** with the appropriate boundary and initial conditions. In section 4.1.3 the numerical results of the inner mean flow are discussed.

Equation (3.19) is parabolic an initial condition is necessary. The initial point of integration is the stagnation point where the outer mean flow has a particular form in Φ_{L}-Ψ_{L} coordinates:

$$\widetilde{U}_b = \sqrt{\frac{4\pi}{\Lambda}\Phi_{\mathrm{L}}}.$$

Thus in this particular case the coefficient m in equation (3.19) is $m = 1/2$ and the equation reduces to a simpler equation with similarity because the function F does not depend on Φ_{L}:

$$F''' + FF'' - F'^2 + 1 = 0, \tag{3.22}$$

with the boundary conditions

$$F(0) = 0, \qquad F'(0) = 0, \qquad F'(\infty) = 1, \tag{3.23}$$

Equation (3.22) is the well known Hiemenz equation which is numerically solved in order to have the behaviour of the inner mean flow close to the stagnation point.

A regular perturbation expansion is used near the stagnation point, where the solution is expanded as a series in Φ_{L} and terms with equal powers of Φ_{L} are collected .

$$F = F_0 + \Phi_{\mathrm{L}} F_1, \tag{3.24}$$

$$m(\Phi_{\mathrm{L}}) = \frac{1}{2} + C\Phi_{\mathrm{L}}. \tag{3.25}$$

The leading order gives the Hiemenz flow equation while the second order gives an equation for F_1 which depends on F_0 and it is numerically solved.

$$F_0''' + F_0 F_0'' - F_0'^2 + 1 = 0, \tag{3.26}$$

$$F_1''' + F_0 F_1'' + F_1 F_0'' - 2F_0' F_1' + 2C - 2F_0'^2 = 2F_0' F_1' - 2F_1' F_0''. \tag{3.27}$$

The total mean flow is given by the composite solution

$$\widetilde{U}^*_{\mathrm{TOT}} = F'^* + \widetilde{U}^* - \widetilde{U}^*_b. \tag{3.28}$$

By scaling by $\widetilde{U}^*_b$ the following is obtained

$$\widetilde{U}_{\mathrm{TOT}} = F' + \frac{\widetilde{U}^*}{\widetilde{U}^*_b} - 1, \tag{3.29}$$

and dividing and multiplying the second term by U^*_∞ the dimensionless total mean flow is given by

$$\widetilde{U}_{\mathrm{TOT}} = F' + \frac{\widetilde{U}}{\widetilde{U}_b} - 1. \tag{3.30}$$

The composite solution for the wall normal velocity component can be obtained in a similar way.

3.1.3 The perturbation flow

Outer perturbation flow

The upstream vortical flow is represented by a convected perturbation of a uniform mean flow U^*_∞, namely the flow upstream is

$$\mathbf{V} = \hat{i} + \epsilon \mathbf{u}_\infty(x_{\mathrm{L}} - t_{\mathrm{L}}, y_{\mathrm{L}}, z_{\mathrm{L}}), \tag{3.31}$$

where $\mathbf{V}$ is the dimensionless velocity vector with components u, v and w along x, y, z and

$$\mathbf{u}_\infty = \hat{\mathbf{u}}^\infty e^{ik(k_{1G}x_{\mathrm{L}} + k_{2G}y_{\mathrm{L}} + k_{3G}z_{\mathrm{L}} - t_{\mathrm{L}})} + c.c., \tag{3.32}$$

with $k = 2\pi L^*/\lambda^*_\Phi$, $k_{1G} = 1$, $k_{2G} = \lambda^*_\Phi/\lambda^*_\Psi$, $k_{3G} = \lambda^*_\Phi/\lambda^*_z$, λ^*_Φ,λ^*_Ψ,λ^*_z are the wave lengths in the streamwise, normal and spanwise directions thus kk_{1G},kk_{2G},kk_{3G} are the dimensionless wavenumber.

The solution for the perturbation flow in the outer region is of the form suggested by **?**, where the flow is given by a two-dimensional steady mean flow and a three-dimensional unsteady small amplitude perturbation flow:

$$\{u, v, w, p\} = \{\widetilde{U}(x_{\mathrm{L}}, y_{\mathrm{L}}), \widetilde{V}(x_{\mathrm{L}}, y_{\mathrm{L}}), 0, \widetilde{P}(x_{\mathrm{L}})\} + \epsilon\{\tilde{u}, \tilde{v}, \tilde{w}, \tilde{p}\}(x_{\mathrm{L}}, y_{\mathrm{L}})e^{ik(k_{3G}z_{\mathrm{L}} - t_{\mathrm{L}})}, \tag{3.33}$$

The solution (3.33) is substituted in the continuity (3.1) and Navier-Stokes equations (3.2) to obtain the following linearised Navier-Stokes equations

$$\nabla \cdot \tilde{\mathbf{u}} = 0, \tag{3.34}$$

$$\frac{\partial \tilde{\mathbf{u}}}{\partial t_{\mathrm{L}}} + \widetilde{\mathbf{U}} \cdot \nabla\tilde{\mathbf{u}} + \tilde{\mathbf{u}} \cdot \nabla\widetilde{\mathbf{U}} = -\nabla\tilde{p} + \frac{1}{R_{\mathrm{L}}}\nabla \cdot (\nabla\tilde{\mathbf{u}}), \tag{3.35}$$

where $\tilde{\mathbf{u}} = \{\tilde{u}, \tilde{v}, \tilde{w}\}$ and $\widetilde{\mathbf{U}} = \{\widetilde{U}, \widetilde{V}\}$.

The general solution to (3.35) suggested by **?** is

$$\tilde{\mathbf{u}} = \nabla\varphi_{\mathrm{L}} + \tilde{\mathbf{u}}_{\mathrm{H}}, \tag{3.36}$$

where $\nabla\varphi_{\mathrm{L}}$ is the part of the perturbation velocity related with the pressure fluctuations and $\tilde{\mathbf{u}}_{\mathrm{H}}$ is the effect of the imposed upstream vorticity field. This is called Helmholtz decomposition and **?** proved the existence and uniqueness of this solution for Navier-Stokes equations. The latter part of the perturbation velocity is necessary because the upstream boundary condition would not be satisfied only by the potential part since upstream the

pressure fluctuations are zero thus the potential is zero and it cannot match the imposed upstream perturbation velocity. The velocity $\tilde{\mathbf{u}}_{\mathrm{H}}$ satisfies the homogeneous equation (without the pressure term). In the case of a flat plate, $\tilde{\mathbf{u}}_{\mathrm{H}}$ coincides with $\mathbf{u}_\infty$ (initial gust) because there is not distortion due to the curvature. This can mathematically be observed in the equations for $\tilde{\mathbf{u}}_{\mathrm{H}}$.

$$\frac{\partial \tilde{\mathbf{u}}_{\mathrm{H}}}{\partial t_{\mathrm{L}}} + \widetilde{\mathbf{U}} \cdot \nabla \tilde{\mathbf{u}}_{\mathrm{H}} + \tilde{\mathbf{u}}_{\mathrm{H}} \cdot \nabla \widetilde{\mathbf{U}} = \frac{1}{R_{\mathrm{L}}} \nabla \cdot (\nabla \tilde{\mathbf{u}}_{\mathrm{H}}). \tag{3.37}$$

The above equation contains the mean flow $\widetilde{\mathbf{U}}$ which for a flat plate is uniform, thus $\tilde{\mathbf{u}}_{\mathrm{H}}$ for a flat plate can only be equal to the initial gust, used as upstream boundary condition. This is the case studied in **?** where the solution in region I is given by (3.1)-(**?**). The velocity must satisfies the continuity equation which in their case becomes the Laplace's equation (3.3)-(**?**) for the perturbation potential.

For the case studied herein the mean flow is given by a uniform flow plus a source flow and therefore its gradient is not zero. Thus there is a distortion in the perturbation velocity field.

From the continuity equation φ_{L} is given by

$$\nabla^2 \varphi_{\mathrm{L}} = -\nabla \cdot \tilde{\mathbf{u}}_{\mathrm{H}}. \tag{3.38}$$

The pressure $\tilde{p}$ is given by

$$\tilde{p} = -\frac{\partial \varphi_{\mathrm{L}}}{\partial t_{\mathrm{L}}} - \widetilde{\mathbf{U}} \cdot \nabla \varphi_{\mathrm{L}} + \frac{1}{R_{\mathrm{L}}} \nabla^2 \varphi_{\mathrm{L}}. \tag{3.39}$$

One of the hypothesis at the beginning stated that $\lambda^* \ll L^*$. Equation (3.37) was obtained by using the outer scale L^* and $1/R_{\mathrm{L}}$ is the small parameter. WKBJ theory is used to obtain the approximated solution of a linear differential equation whose highest derivative is multiplied by a small parameter (**?**). In this case the small parameter used to obtain the solution is absent from the equations but the scale of perturbation motion is much smaller than the characteristic length of mean flow. Moreover the spatial scale of the perturbation is much smaller than L^* which is used in analogy to the application of WKBJ theory to classical ordinary differential equations, where the equations are initially scaled by the larger scale. This case is very similar to that one of **?** (page 223) where there is not a small parameter in the equations, then it is not obvious how to use WKBJ theory. By using WKBJ theory the solution to (3.37) can be taken of the form

$$\tilde{\mathbf{u}}_{\mathrm{H}} = e^{iks} \left(\tilde{\mathbf{u}}_0 + \frac{1}{ik} \tilde{\mathbf{u}}_1 + ... \right) e^{ik(k_{3G} z_{\mathrm{L}} - t_{\mathrm{L}})}, \tag{3.40}$$

where $k = 2\pi L^*/\lambda^*_\Phi \gg 1$. By substituting (3.40) in (3.37) and equating coefficients of inverse powers of k, the following are obtained:

$$1 - \widetilde{\mathbf{U}} \cdot \nabla s = -\frac{i}{R_{\lambda_\Phi}} (\nabla s \cdot \nabla s + k_{3G}^2), \tag{3.41}$$

$$\widetilde{\mathbf{U}} \cdot \nabla \tilde{\mathbf{u}}_0 - \frac{2i}{R_{\lambda_\Phi}} \nabla s \cdot \nabla \tilde{\mathbf{u}}_0 - \frac{i}{R_{\lambda_\Phi}} \tilde{\mathbf{u}}_0 \nabla^2 s + \tilde{\mathbf{u}}_0 \cdot \nabla \widetilde{\mathbf{U}} = 0, \tag{3.42}$$

where $R_{\lambda_\Phi} = R_\mathrm{L}/k = \mathcal{O}(1)$.

It has to be remarked that in obtaining equation (3.41) the following assumptions have been made:

- λ^*_Φ,λ^*_Ψ,$\lambda^*_z \ll L^*$ namely the wavelengths of the disturbance in the three spacial directions are all of the same order and they are all smaller than the characteristic length of the body L^*.
- R_{λ_Φ} is of order 1. This assumption permitted to use WKBJ theory to expand the solution for the velocity as in (3.40). This theory is used to obtain the approximated solution of partial differential equations whose the highest derivative is multiplied by a small parameter. The equation for $\tilde{\mathbf{u}}_\mathrm{H}$ is (3.37) where $\tilde{\mathbf{u}}_\mathrm{H}$ is a function of only $x_\mathrm{L} - y_\mathrm{L}$, the ∇ operator is in coordinates $x_\mathrm{L} - y_\mathrm{L}$ and t_L is the time scaled by the mean flow velocity and L^*. The small parameter in this equation is $1/R_\mathrm{L}$. In WKBJ theory the solution expands as in (3.40) where the phase is multiplied by a large parameter, which should be the inverse of the small parameter in the equation (in this case the Reynolds number R_L). We actually choose to multiply the phase by k, following **?** .

It is convenient to use the optimal coordinates. Here, in the outer region, the potential and stream function used are Φ_L and Ψ_L associated with the outer mean flow $\widetilde{\mathbf{U}}$. A new function is introduced

$$s_{0L} = \frac{2}{R_{\lambda_\Phi}} s + i(\Phi_\mathrm{L} - \Phi_{\mathrm{L}0}), \tag{3.43}$$

where $\Phi_{\mathrm{L}0}$ is an arbitrary constant and $s_{0L} = s^*_0/L^*$. Then (3.41) becomes

$$\left(\frac{\partial s_{0L}}{\partial \Phi_\mathrm{L}}\right)^2 + \left(\frac{\partial s_{0L}}{\partial \Psi_\mathrm{L}}\right)^2 = Q^2(\Phi_\mathrm{L}, \Psi_\mathrm{L}), \tag{3.44}$$

where

$$Q^2 = \frac{4i}{R_{\lambda_\Phi}|\widetilde{\mathbf{U}}|^2}\left(1 + \frac{ik^2_{3G}}{R_{\lambda_\Phi}}\right) - 1,$$

with $|\widetilde{\mathbf{U}}| = |\nabla\Phi_\mathrm{L}|$. Equation (3.44) is called Eikonal equation.

The boundary conditions on all the four boundaries are taken as equation (3.27) in **?** which is the solution for equation (3.41) for a constant mean flow, thus it can be used as the solution far from the body, where the mean flow is uniform. The solution is

$$s = k_{2G} y_\mathrm{L} + \left[\sqrt{\frac{1}{4}R^2_{\lambda_\Phi} Q^2 - k^2_{2G}} - \frac{1}{2}R_{\lambda_\Phi} i\right](x_\mathrm{L} - x_{L0}). \tag{3.45}$$

By substituting Q^2 for $|\widetilde{\mathbf{U}}|$ constant in the above equation the following is obtained:

$$s = k_{2G} y_\mathrm{L} + \left[\sqrt{iR_{\lambda_\Phi} - k^2_{3G} - \frac{R^2_{\lambda_\Phi}}{4} - k^2_{2G}} - \frac{1}{2}R_{\lambda_\Phi} i\right](x_\mathrm{L} - x_{L0}).$$

The problem is simplified by considering an inviscid outer perturbation flow. Under this assumption new hypothesis can be introduced:

1. $\delta^* \ll \lambda_z^*$, where δ^* is he boundary layer thickness.
2. $\lambda_z^* \ll \lambda_\Phi^* \ll L^*$ and $\lambda_z^*/\lambda_\Phi^* = \mathcal{O}(k_\Phi)$, $\lambda_\Phi^*/L^* = \mathcal{O}(k_\Phi)$, $\lambda_z^*/L^* = \mathcal{O}(k_\Phi^2)$, $\lambda_z^*/\lambda_\Psi^* = \mathcal{O}(1)$ where k_Φ is the dimensionless streamwise wavenumber given by $2\pi\Lambda_z^*/\lambda_\Phi^*$, which under this hypothesis is small.

Each hypothesis has an important physical meaning.

- $\delta^* \ll \lambda_z^*$. This ratio between the boundary layer thickness and the spanwise wavelength is taken as in region II of **?**. This first implies that there is not displacement, like in region I of **?**, thus the streamlines are only deflected by the actual body and not by the additional displacement due to boundary layer. If displacement effect was considered the streamlines external to the boundary layer would be deflected upward of a distance which is exactly the boundary layer thickness. The displacement effect gives rise to the concept of an effective body, namely the free stream sees the contour of the boundary layer as if it was the body. In this region the outer flow is still inviscid, which is in fact the case that is considered here and the boundary region equations simplify to the boundary layer equations.

- $\lambda_z^* \ll \lambda_\Phi^*$. This ratio between the two wavelengths in the spanwise and streamwise directions is the disturbance hypothesis, also taken in **?**. It was experimentally demonstrated that the disturbances associated with laminar streaks evolves over distances which are larger in the streamwise wavelength than in the normal and spanwise wavelengths. Under this assumption the dimensionless streamwise wavenumber k_Φ is small and during the analysis of the inner region it will be seen that this allows to obtain parabolic equations inside the boundary layer.

- $\lambda_\Phi^* \ll L^*$. This ratio between the characteristic length of the body and the streamwise wavelength allowed to use WKBJ method during the analysis of the outer flow, as already stated.

After all these considerations, the solution to the Eikonal equation is the (3.26) in **?**, which is valid in the inviscid limit

$$s_{0L} = \frac{2}{R_{\lambda_\Phi}} \left[k_{2G}\Psi_{\mathrm{L}} + \int_{\Phi_{\mathrm{L}0}}^{\Phi_{\mathrm{L}}} \frac{1}{|\widetilde{\mathbf{U}}|^2}\, d\Phi'_{\mathrm{L}} \right] + i(\Phi_{\mathrm{L}} - \Phi_{\mathrm{L}0}). \tag{3.46}$$

It can be easily demonstrated that the solution 3.46 satisfies both the Eikonal equation 3.44 and equation 3.41 in the limit of $R_{\lambda_\Phi} \to \infty$ and in a region far from the stagnation point, where $|\widetilde{\mathbf{U}}|^2$ is of order 1. In fact the Eikonal equation becomes

$$\left(\frac{\partial s_{0L}}{\partial \Phi_{\mathrm{L}}}\right)^2 + \left(\frac{\partial s_{0L}}{\partial \Psi_{\mathrm{L}}}\right)^2 = -1, \tag{3.47}$$

and s_{0L} in the inviscid limit is

$$s_{0L} = i(\Phi_{\mathrm{L}} - \Phi_{\mathrm{L}0}),$$

which satisfies 3.47. Equation 3.41 in the inviscid limit of $R_{\lambda_\Phi} \to \infty$ and in $\Phi_L - \Psi_L$ coordinates becomes

$$1 - |\widetilde{\mathbf{U}}|^2 \frac{\partial s}{\partial \Phi_L} = 0, \tag{3.48}$$

because the inviscid outer mean flow is parallel to the streamlines (its only component is along Φ). Equation (3.48) is satisfied by the solution

$$s = k_{2G}\Psi_L + \int_{\Phi_{L0}}^{\Phi_L} \frac{1}{|\widetilde{\mathbf{U}}|^2}\, d\Phi'_L. \tag{3.49}$$

The streamwise coordinate to be used is $\bar{\Phi} = k_\Phi \Phi$ which is the streamwise coordinate scaled by the streamwise disturbance wavelength. The right scale for the disturbance is $\bar{\Phi}$ because the disturbance associated with laminar streaks evolves over distances which are larger in the wavelength along Φ^* than in those ones along Ψ^*, z^*. The Φ^* coordinate is therefore scaled by λ^*_Φ. This can be better understood by remembering that

$$\widetilde{U} = \frac{\partial \Phi}{\partial x},$$

and since x is rescaled by λ^*_Φ also the potential function must be rescaled with the same quantity in order to have the velocity of order 1. Time is scaled in the same way because streaks modulate slowly in time. The normal coordinate Ψ is scaled by the shortest disturbance wavelength λ^*_z. The solution for the phase factor in the new scales is

$$s = k_\Psi \Psi + \int_{\bar{\Phi}}^{\bar{\Phi}} \frac{1}{|\widetilde{\mathbf{U}}|^2}\, d\bar{\Phi}', \tag{3.50}$$

where k_ψ is the dimensionless normal wavenumber.

Once the solution for s_{0L} (then for s) is obtained, a solution for $\tilde{\mathbf{u}}_0$ can be found. The coordinates are changed as for the phase s and the following is obtained:

$$\widetilde{\mathbf{U}} \cdot |\widetilde{\mathbf{U}}| \widetilde{\nabla} \tilde{\mathbf{u}}_0 - \frac{2i}{R_{\lambda_\Phi}} |\widetilde{\mathbf{U}}|^2 \widetilde{\nabla} s \cdot \widetilde{\nabla} \tilde{\mathbf{u}}_0 - \frac{i}{R_{\lambda_\Phi}} \tilde{\mathbf{u}}_0 |\widetilde{\mathbf{U}}|^2 \widetilde{\nabla}^2 s + \tilde{\mathbf{u}}_0 \cdot |\widetilde{\mathbf{U}}| \widetilde{\nabla} \widetilde{\mathbf{U}} = 0, \tag{3.51}$$

where the $\widetilde{\nabla}$ operator is in (Φ_L,Ψ_L) coordinates and the boundary conditions are

$$\tilde{\mathbf{u}}_0 e^{iks} \to \hat{\mathbf{u}}^\infty e^{ik(k_{1G}x_L + k_{2G}y_L)} \qquad \text{as} \quad \Psi_L \to \infty, \tag{3.52}$$

$$\tilde{\mathbf{u}}_0 e^{iks} \to \hat{\mathbf{u}}^\infty e^{ik(k_{1G}x_L + k_{2G}y_L)} \qquad \text{as} \quad \Psi_L \to -\infty. \tag{3.53}$$

WKBJ theory is employed again to find the solution for the perturbation potential:

$$\varphi_L = \frac{e^{iks}}{k}\left(\varphi_0 + \frac{1}{ik}\varphi_1 + ...\right) e^{ik(k_{3G}z_L - t_L)}, \tag{3.54}$$

and φ_0 is found by substituting the above equation into the continuity equation (3.38):

$$\varphi_0 = \frac{i\hat{\mathbf{u}}^\infty \cdot (\nabla s + k_{3G}\hat{k})}{\nabla^2 s + k_{3G}^2}. \tag{3.55}$$

where $\hat{k}$ is the unit vector along the spanwise direction.
The total outer perturbation velocity is found by equation (3.36).
The outer perturbation pressure is given by

$$\tilde{p} = \tilde{p}_e(x_{\text{L}}, y_{\text{L}})e^{ik(k_{3G}z_{\text{L}} - t_{\text{L}})}, \tag{3.56}$$

and it is found by the outer perturbation potential as

$$\tilde{p} = -\frac{\partial \varphi_{\text{L}}}{\partial t_{\text{L}}} - \widetilde{\mathbf{U}} \cdot \nabla \varphi_{\text{L}} + \frac{1}{R_{\text{L}}}\nabla^2 \varphi_{\text{L}}. \tag{3.57}$$

The above formula is shown to be valid by **?**. The outer perturbation pressure is of order k_Φ as the inner perturbation pressure (leib-wundrow-goldstein-1999). This is an interesting result because it means that the inner pressure matches the outer pressure . The pressure is written as

$$\tilde{p}_e = k_\Phi \tilde{p}_0.$$

where $\tilde{p}_0$ is of order 1 and it is given by

$$\tilde{p}_0 = i\varphi_0 - |\widetilde{\mathbf{U}}|^2 \frac{\partial \varphi_0}{\partial \bar{\Phi}}. \tag{3.58}$$

3.1.4 Inner perturbation flow

Boundary region equations

The solution in the inner region is of the form suggested by **?**:

$$\{w_\Phi, w_\Psi, w_z, p\} = \{U(\bar{\Phi}, \eta), V(\bar{\Phi}, \eta), 0, P(\bar{\Phi})\} + \epsilon \left\{ \bar{u}_0, \sqrt{\frac{2\bar{\Phi}k_\Phi}{R}}\bar{v}_0, \bar{w}_0, \frac{ik_z}{\sqrt{Rk_\Phi}}\sqrt{\frac{k_\Phi}{R}}\bar{p} \right\} (\bar{\Phi}, \eta)e^{i(k_z z - k_\Phi t)}, \tag{3.59}$$

where $\bar{\Phi}$ is of order 1, η is of order 1, $k_z = 2\pi$ is the spanwise wavenumber, U, V are the components of the 2-dimensional mean flow, $\bar{u}_0, \bar{v}_0, \bar{w}_0$ are the components of the 3-dimensional perturbation flow. Navier-Stokes equations in optimal coordinates are

$$\widetilde{U}\frac{\partial w_\Phi}{\partial \Phi} + \widetilde{U}\frac{\partial w_\Psi}{\partial \Psi} + \frac{\partial w_z}{\partial z} = 0, \tag{3.60}$$

$$\begin{aligned} &\frac{1}{\widetilde{U}^2}\frac{\partial w_\Phi}{\partial t} + w_\Phi \frac{\partial w_\Phi}{\partial \Phi} + w_\Psi \frac{\partial w_\Phi}{\partial \Psi} + \frac{1}{\widetilde{U}} w_z \frac{\partial w_\Phi}{\partial z} + \frac{\partial \log \widetilde{U}}{\partial \Phi}\left(w_\Phi^2 + w_\Psi^2\right) = \\ &-\frac{1}{\widetilde{U}^2}\frac{\partial p}{\partial \Phi} + \frac{1}{R}\left[\frac{\partial^2 w_\Phi}{\partial \Phi^2} + \frac{\partial^2 w_\Phi}{\partial \Psi^2} + \frac{1}{\widetilde{U}^2}\frac{\partial^2 w_\Phi}{\partial z^2} - 2\frac{\partial \ln \widetilde{U}}{\partial \Psi}\left(\frac{\partial w_\Psi}{\partial \Phi} - \frac{\partial w_\Phi}{\partial \Psi}\right) - \frac{2}{\widetilde{U}}\frac{\partial \ln \widetilde{U}}{\partial \Phi}\frac{\partial w_z}{\partial z}\right], \end{aligned} \tag{3.61}$$

$$\frac{1}{\widetilde{U}^2}\frac{\partial w_\Psi}{\partial t} + w_\Phi\frac{\partial w_\Psi}{\partial \Phi} + w_\Psi\frac{\partial w_\Psi}{\partial \Psi} + \frac{1}{\widetilde{U}}w_z\frac{\partial w_\Psi}{\partial z} + \frac{\partial \log \widetilde{U}}{\partial \Psi}\left(w_\Phi^2 + w_\Psi^2\right) =$$
$$-\frac{1}{\widetilde{U}^2}\frac{\partial p}{\partial \Psi} + \frac{1}{R}\left[\frac{\partial^2 w_\Psi}{\partial \Phi^2} + \frac{\partial^2 w_\Psi}{\partial \Psi^2} + \frac{1}{\widetilde{U}^2}\frac{\partial^2 w_\Psi}{\partial z^2} + 2\frac{\partial \ln \widetilde{U}}{\partial \Phi}\left(\frac{\partial w_\Psi}{\partial \Phi} - \frac{\partial w_\Phi}{\partial \Psi}\right) - \frac{2}{\widetilde{U}}\frac{\partial \ln \widetilde{U}}{\partial \Psi}\frac{\partial w_z}{\partial z}\right], \tag{3.62}$$

$$\frac{1}{\widetilde{U}^2}\frac{\partial w_z}{\partial t} + w_\Phi\frac{\partial w_z}{\partial \Phi} + w_\Psi\frac{\partial w_z}{\partial \Psi} + \frac{1}{\widetilde{U}}w_z\frac{\partial w_z}{\partial z} + w_z\left(w_\Phi\frac{\partial \log \widetilde{U}}{\partial \Phi} + w_\Psi\frac{\partial \log \widetilde{U}}{\partial \Psi}\right) =$$
$$-\frac{1}{\widetilde{U}^3}\frac{\partial p}{\partial z} + \frac{1}{R}\left[\frac{\partial^2 w_z}{\partial \Phi^2} + \frac{\partial^2 w_z}{\partial \Psi^2} + \frac{1}{\widetilde{U}^2}\frac{\partial^2 w_z}{\partial z^2} + \frac{w_z}{\widetilde{U}}\left(\frac{\partial^2 \widetilde{U}}{\partial \Phi^2} + \frac{\partial^2 \widetilde{U}}{\partial \Psi^2}\right) + 2\left(\frac{\partial w_z}{\partial \Phi}\frac{\partial \ln \widetilde{U}}{\partial \Phi} + \frac{\partial w_z}{\partial \Psi}\frac{\partial \ln \widetilde{U}}{\partial \Psi}\right)\right], \tag{3.63}$$

By substituting (3.59) in (3.60)-(3.63), taking the outer inviscid mean velocity along the body surface and putting together terms of order ϵ, the following are obtained:

$$\frac{\partial \bar{u}_0}{\partial \bar{\Phi}} - \frac{\partial \bar{u}_0}{\partial \eta}\frac{\eta}{2\bar{\Phi}} + \frac{\partial \bar{v}_0}{\partial \eta} + \frac{\bar{w}_0}{\widetilde{U}_b}\frac{ik_z}{k_\Phi} = 0. \tag{3.64}$$

Since in the boundary region k_z is of order 1, $\bar{u}_0$ and $\bar{v}_0$ need to be rescaled:

$$\bar{u}_0 = \frac{ik_z}{k_\Phi}\bar{u}, \qquad \bar{v}_0 = \frac{ik_z}{k_\Phi}\bar{v}, \qquad \bar{w}_0 = \bar{w}, \tag{3.65}$$

where $\bar{u}$, $\bar{v}$ and $\bar{w}$ are now the functions to find. Thus (3.64) becomes

$$\frac{\partial \bar{u}}{\partial \bar{\Phi}} - \frac{\partial \bar{u}}{\partial \eta}\frac{\eta}{2\bar{\Phi}} + \frac{\partial \bar{v}}{\partial \eta} + \frac{\bar{w}}{\widetilde{U}_b} = 0, \tag{3.66}$$

$$-\frac{i\bar{u}}{\widetilde{U}_b^2} + \frac{\partial F}{\partial \eta}\frac{\partial \bar{u}}{\partial \bar{\Phi}} + \bar{u}\frac{\partial^2 F}{\partial \bar{\Phi}\partial \eta} - \bar{u}\frac{\partial^2 F}{\partial \eta^2}\frac{\eta}{2\bar{\Phi}} - \frac{\partial F}{\partial \bar{\Phi}}\frac{\partial \bar{u}}{\partial \eta} - \frac{F}{2\bar{\Phi}}\frac{\partial \bar{u}}{\partial \eta} + \bar{v}\frac{\partial^2 F}{\partial \eta^2} = \frac{1}{2\bar{\Phi}}\frac{\partial^2 \bar{u}}{\partial \eta^2} - \frac{\kappa^2}{\widetilde{U}_b^2}\bar{u}, \tag{3.67}$$

$$\begin{aligned}
&-\frac{i\bar{v}}{\widetilde{U}_b^2} + \frac{\partial F}{\partial \eta}\frac{\partial \bar{v}}{\partial \bar{\Phi}} - \frac{F}{2\bar{\Phi}}\frac{\partial \bar{v}}{\partial \eta} + \frac{1}{2\bar{\Phi}}\frac{\partial}{\partial \eta}\left(\eta\frac{\partial F}{\partial \eta}\right)\bar{v} - \\
&-\bar{u}\left\{\frac{1}{(2\bar{\Phi})^2}\left[\eta\frac{\partial}{\partial \eta}\left(\eta\frac{\partial F}{\partial \eta}\right) - F\right] + \frac{\partial^2 F}{\partial \bar{\Phi}^2} - \frac{\eta}{\bar{\Phi}}\frac{\partial^2 F}{\partial \bar{\Phi}\partial \eta} + \frac{1}{\bar{\Phi}}\frac{\partial F}{\partial \bar{\Phi}}\right\} - \\
&-\frac{\partial F}{\partial \bar{\Phi}}\frac{\partial \bar{v}}{\partial \eta} - \bar{v}\frac{\partial^2 F}{\partial \bar{\Phi}\partial \eta} = -\frac{1}{\widetilde{U}_b^2}\frac{1}{2\bar{\Phi}}\frac{\partial \bar{p}}{\partial \eta} + \frac{1}{2\bar{\Phi}}\frac{\partial^2 \bar{v}}{\partial \eta^2} - \frac{1}{\widetilde{U}_b^2}\kappa^2\bar{v},
\end{aligned} \tag{3.68}$$

$$-\frac{i\bar{w}}{\widetilde{U}_b^2} + \frac{\partial F}{\partial \eta}\frac{\partial \bar{w}}{\partial \bar{\Phi}} - \frac{\partial F}{\partial \bar{\Phi}}\frac{\partial \bar{w}}{\partial \eta} - \frac{F}{2\bar{\Phi}}\frac{\partial \bar{w}}{\partial \eta} = \frac{\kappa^2}{\widetilde{U}_b^3}\bar{p} + \frac{\partial^2 \bar{w}}{\partial \eta^2}\frac{1}{2\bar{\Phi}} - \frac{1}{\widetilde{U}_b^2}\kappa^2\bar{w}. \tag{3.69}$$

In (3.67), (3.68) and (3.69) terms of the smallest power of k_Φ are put together and

$$\kappa = \frac{k_z}{\sqrt{Rk_\Phi}} = \mathcal{O}(1).$$

Equations (3.66)-(3.69) need 7 boundary conditions in η. Three of them are the no slip conditions for $\bar{u}$, $\bar{v}$ and $\bar{w}$, namely

$$\bar{u} = \bar{v} = \bar{w} = 0, \qquad \text{at} \quad \eta = 0. \tag{3.70}$$

The streamwise perturbation velocity $\bar{u}$ inside the boundary layer is of order $1/k_\Phi$ (see (3.59)), while the streamwise perturbation velocity $\tilde{u}$ outside the boundary layer is of order 1 (see (3.33)). Since $\bar{u}$ is larger than $\tilde{u}$ it can not match with the outer solution for $\eta \to \infty$, then

$$\bar{u} \to 0 \qquad \text{as} \quad \eta \to \infty. \tag{3.71}$$

The perturbation velocities $\bar{v}$ and $\bar{w}$ can match the outer perturbation solutions $\tilde{v}$ and $\tilde{w}$ because they are both of order 1, then

$$\bar{v} \to -i\frac{\tilde{v}}{\kappa\widetilde{U}_b\sqrt{2\bar{\Phi}}} \qquad \text{as} \quad \eta \to \infty, \tag{3.72}$$

$$\bar{w} \to \frac{\tilde{w}}{\widetilde{U}_b} \qquad \text{as} \quad \eta \to \infty. \tag{3.73}$$

The order of the outer perturbation pressure around the Rankine body is the same of the inner perturbation pressure, thus at large distance from the body the inner pressure matches the outer perturbation pressure:

$$\bar{p} \to \frac{k_\Phi}{i\kappa}\left(\frac{R}{k_\Phi}\right)^{1/2}\tilde{p}_0 \qquad \text{as} \quad \eta \to \infty. \tag{3.74}$$

The initial conditions for boundary region equations are valid in the region where $\bar{\Phi} \ll 1$ and they are obtained in the form of a power series.

4. RESULTS AND DISCUSSION

4.1 Mean flow solution

4.1.1 Mean pressure

The mean pressure coefficient is defined as

$$C_p = 1 - \widetilde{U}^2.$$

The pressure changes along the body surface because of the curvature and it is studied as a function of s. The behavior of C_p is shown in figure 4.1. At the stagnation point $C_p = 1$ and since there is symmetry the slope of the curve is zero. Then the fluid accelerates and the pressure decreases until the fluid starts to decelerate and the pressure increases. This result is also obtained by **?** and his curve and the one numerically obtained perfectly overlap as shown in figure 4.1.

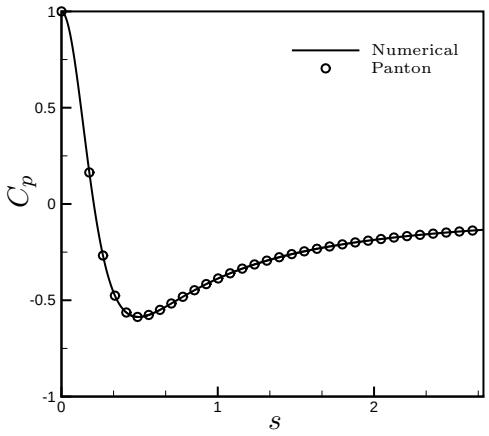

Fig. 4.1: Mean pressure gradient as a function of s along the body.

4.1.2 Boundary layer thickness

The boundary layer thickness is the distance from the body to a point where the velocity reaches the free stream velocity value, in particular it is defined as the distance where $u = 0.99U_\infty$. This distance can be numerically found by the definition of η, which is the

inner variable used to find the solution in the viscous boundary layer. In optimal coordinates η is define as

$$\eta = \Psi_{\mathrm{L}} \sqrt{\frac{R_{\mathrm{L}}}{2\Phi_{\mathrm{L}}}}.$$

Once obtained the solution of the inner mean flow (next section) the value of η where the velocity has the free stream value can be found for every streamwise coordinate Φ_{L} and this value is supposed to be different on the curvature where the solution is not similar. Two important checks can be done analytically and numerically: at the stagnation point and downstream, where the flow is uniform, the boundary layer thickness is well known. In particular at the stagnation point the potential and stream function are:

$$\Psi_{\mathrm{L}} = \frac{2\pi}{\Lambda} x'_{\mathrm{L}} y'_{\mathrm{L}}, \qquad \Phi_{\mathrm{L}} = \frac{\pi x'^2_{\mathrm{L}}}{\Lambda},$$

where the coordinates with prime are the ones used at the stagnation point (figure 3.1). By substituting the two above equations in the definition of η the following is obtained:

$$\eta = y'_{\mathrm{L}} \sqrt{\frac{2\pi R_{\mathrm{L}}}{\Lambda}}.$$

Thus the boundary layer thickness for the stagnation point is constant and equal to:

$$y'_{\mathrm{L}} = \eta_\delta \sqrt{\frac{\Lambda}{2\pi R_{\mathrm{L}}}},$$

where η_δ is the value of η where the velocity is 0.99 and it is numerically found to be $\eta_\delta = 2.4$. This result is in agreement with **?**:

$$\delta^* = 2.4 \sqrt{\frac{\nu^*}{a^*}},$$

where $a^* = \alpha U^*_\infty / L^*$, $\alpha = 2\pi/\Lambda$. By substituting the value of a^* in the boundary layer thickness found by **?** it is obtained:

$$\delta_{\mathrm{L}} = 2.4 \sqrt{\frac{\Lambda}{2\pi R_{\mathrm{L}}}},$$

which is the thickness previously found. The same analytical check can be done downstream where the potential and stream fnction are:

$$\Psi_{\mathrm{L}} = y_{\mathrm{L}}, \qquad \Phi_{\mathrm{L}} = x_{\mathrm{L}},$$

and therefore

$$y_{\mathrm{L}} = \eta_\delta \sqrt{\frac{2x_{\mathrm{L}}}{R_{\mathrm{L}}}}.$$

Downstream the boundary layer grows as $x_{\mathrm{L}}^{1/2}$. On the body is no possible to find analytically the boundary layer thickness since the expressions of the potential and stream

function are more complicated. Therefore, the boundary layer thickness is numerically evaluated and its value is compared with Hiemenz boundary layer at the stagnation point and Blasius boundary layer downstream.

The behavior of the boundary layer thickness along the body is shown in figure 4.3. At the stagnation point, the Hiemenz boundary layer is constant because there is a perfect balance between the wall-normal viscous diffusion, which lets the boundary layer thickness increase and the favourable pressure gradient, which lets the boundary layer thickness decrease. Downstream the pressure gradient effect never overcomes the wall-normal diffusion and eventually wall-normal diffusion takes over completely.

4.1.3 Inner mean velocity

In this section the finite difference solution of the steady mean flow equation in optimal coordinates is presented. Figure 4.2 shows the composite solution for the total mean flow given by equation (3.30) at $s = 1.48$. In figure 4.3 the profiles of the velocity are shown at different positions on the body. At each position the velocity reaches a different free stream value, as expected since the outer mean velocity is not constant. The point where the velocity has the free stream value increases following the boundary layer thickness.

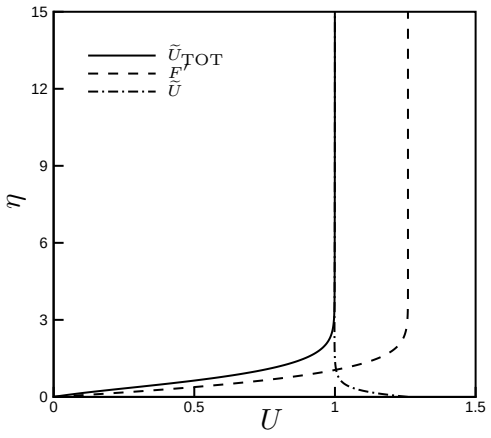

Fig. 4.2: Composite solution of the mean flow.

4.2 Outer flow solution

Figure 4.4 shows the outer perturbation potential at different streamlines. It is the contribution to the total perturbation velocity due to the body therefore it is zero at large distance from the body ($\Psi = 5$). Its behaviour changes by approaching the body. Along the streamline $\Psi = 1$ the potential is zero upstream and downstream where the mean flow is uniform and it increases on the body where the mean flow accelerates. This behaviour is more evident along the streamline closer to the body ($\Psi = 0.09$), where the potential increases, then it rapidly decreases and it increases again to reach a constant value which

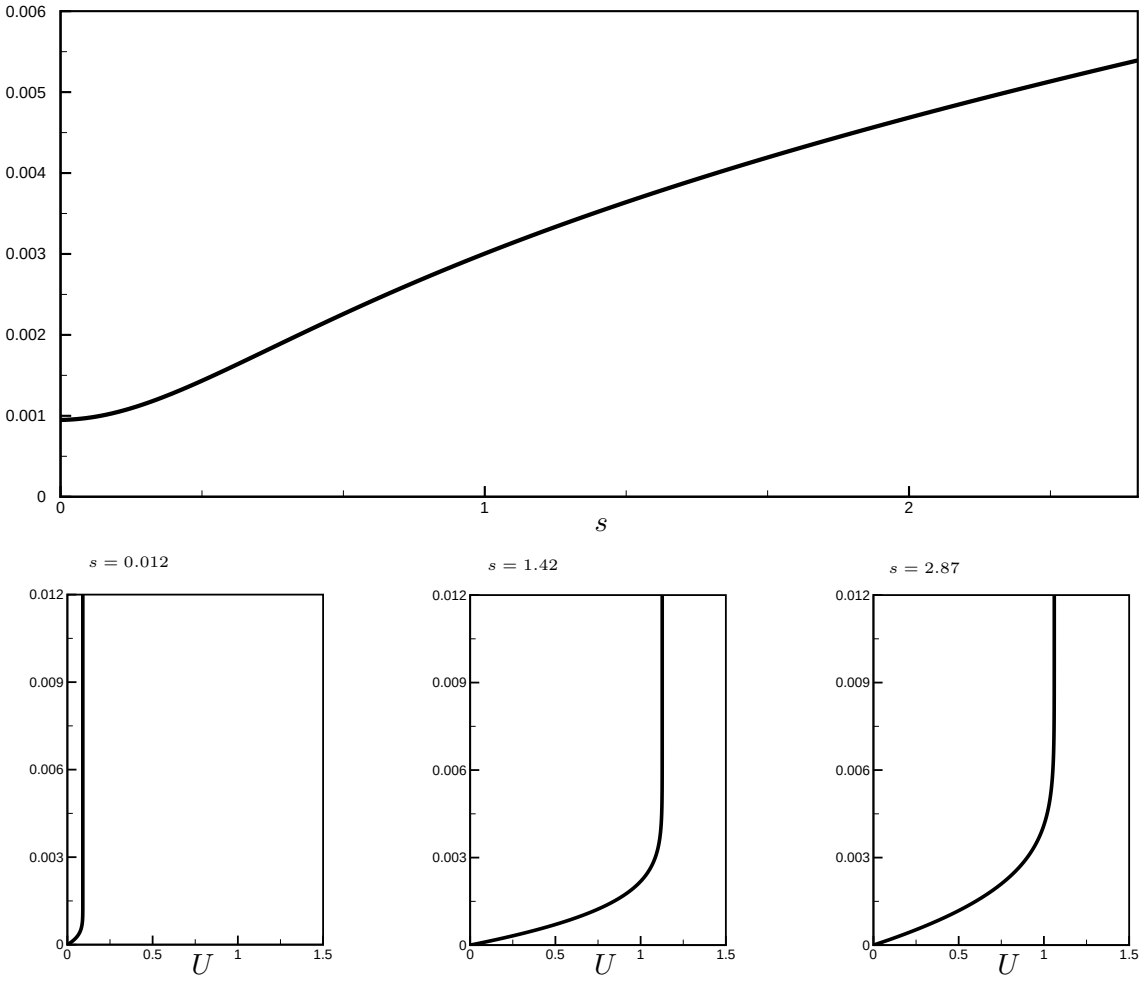

Fig. 4.3: Boundary layer thickness as a function of s (top) and inner mean velocity profiles at different positions on the body (bottom).

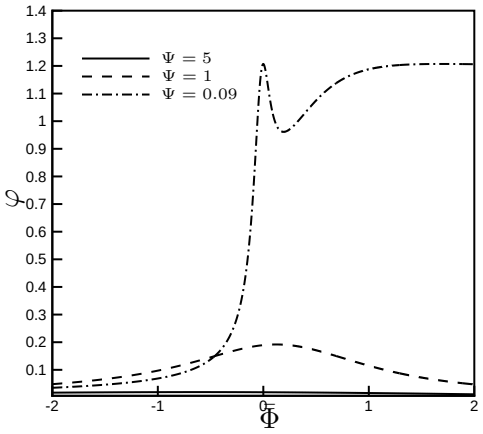

Fig. 4.4: Outer perturbation potential.

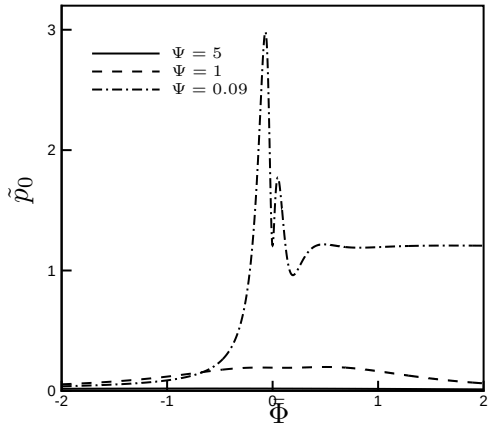

Fig. 4.5: Outer perturbation pressure.

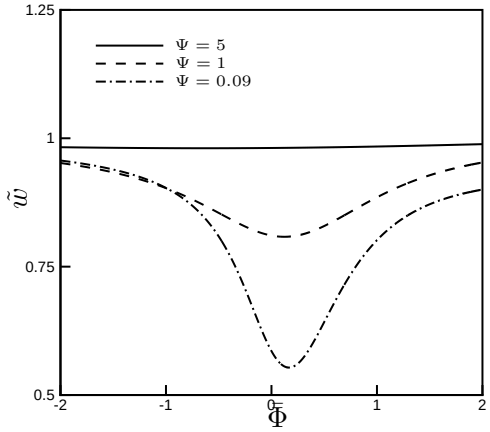

Fig. 4.6: Outer perturbation velocity.

is kept downstream where the flow is parallel. Figure 4.5 shows the outer perturbation pressure which is related to the outer perturbation potential. The pressure is zero at large distance from the body ($\Psi = 5$), but it changes by approaching the body. Along the streamline $\Psi = 1$ it is zero upstream and downstream where the mean flow is uniform and it varies when the flow accelerates. At $\Psi = 0.09$ the pressure is zero upstream, then it varies on the body and it is constant downstream where the flow is uniform. Figure 4.6 shows the behavior of the spanwise outer perturbation velocity component at different streamlines. Far from the body it has the same constant value as the initial gust. At $\Psi = 1$ it is constant upstream and downstream where the mean flow is uniform and it decreases by approaching the body. This behaviour is more evident at $\Psi = 0.09$ closer to the body. The other two velocity components have a similar behaviour.

4.3 Boundary region solution

Figures 4.7 and 4.8 show the amplitude of the streamwise and spanwise velocity components at different values of the streamwise coordinate $\bar{\Phi}$. The effect of the pressure gradient is to modify the streaks which do not have a single peak as in the flat-plate boundary layer. The shape of the streamwise velocity amplitude is different from the results of **?** and this is more evident at small $\bar{\Phi}$. The streaks are initially amplified and then they decay downstream. The behaviour of the spanwise velocity amplitude is due to the free-stream matching requirements. The effect of κ on the streaks at $\bar{\Phi} = 0.5$ is shown in figure 4.9. As κ decreases the streamwise velocity amplitude increases.

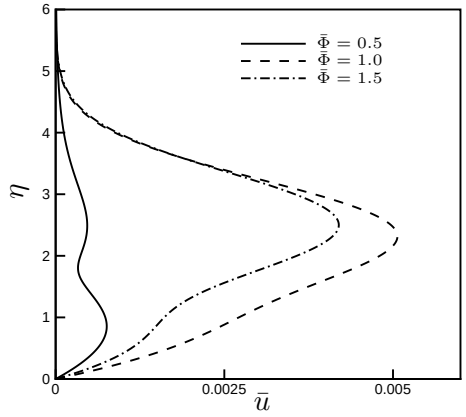

Fig. 4.7: Profile of streamwise perturbation velocity $\bar{u}$ at the indicated values of $\bar{\Phi}$.

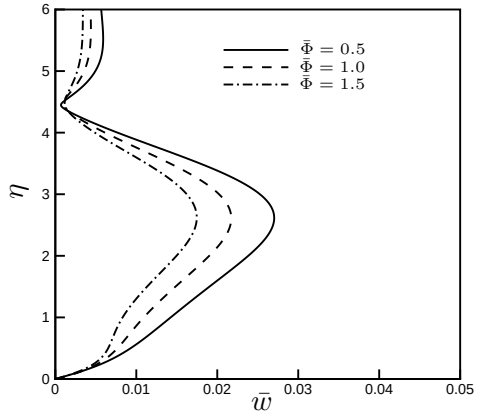

Fig. 4.8: Profile of spanwise perturbation velocity $\bar{w}$ at the indicated values of $\bar{\Phi}$.

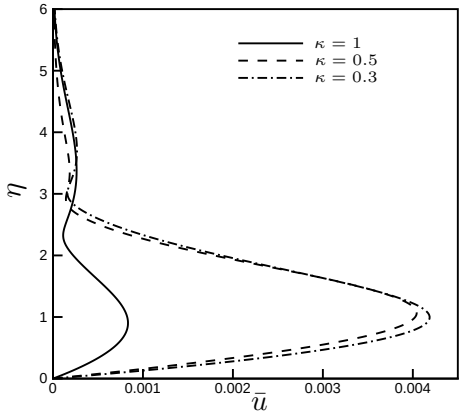

Fig. 4.9: Profile of streamwise perturbation velocity $\bar{u}$ at the indicated values of κ and $\bar{\Phi} = 0.5$.

5. CONCLUSIONS

The downstream evolution of a perturbed incompressible flow at high Reynolds numbers around a Rankine body has been analyzed. Far from the body the flow is decomposed in a mean flow and a perturbation flow. The first one is given by a uniform flow which encounters a source flow. The solution for the outer perturbation flow is found by using WKBJ theory, which returns the phase and the amplitude of the perturbation velocity and consequently the perturbation pressure. The viscous effects in the outer perturbation flow are neglected.

In the unsteady boundary layer region the mean flow satisfies the steady nonlinear mean flow equations without similarity while the perturbation flow is governed by the linearized unsteady boundary region equations in new suitable coordinates. The boundary region equations satisfy appropriate boundary conditions derived from matching with the solution in the outer region and no-slip condition at the wall. Initial conditions for boundary layer equations have been derived in terms of a power series and by considering that at the stagnation point the inner mean flow is the well known Hiemenz flow.

The effect of the mean pressure gradient and the streamwise wavenumber on the streamwise velocity profile has been analyzed. It has also been demonstrated that the inner perturbation pressure matches the outer perturbation pressure which has a very important role in the boundary layer dynamics.

5.1 Future work

The rigorous mathematical approach used in this work could be useful to extend the results to more complex cases. Some ideas have already been developed.

- Considering the streamwise wavelength of the same order of the characteristic length of the body to generalise the results of the outer perturbation flow.
- Studying the effects of viscosity on the outer perturbation flow and how these effects change the solution inside the boundary layer.
- Studying the evolution of order-one disturbances by solving the nonlinear boundary-region equations.
- Using nonlinear streaks as base flow to study secondary instability.
- Studying the perturbed flow around a wedge body. In this case there would be Falkner-Skan boundary layer with self similar equations along the entire body.

APPENDIX

A. DERIVATION OF CONTINUITY AND NAVIER-STOKES EQUATIONS IN OPTIMAL COORDINATES

Since the body is not a flat plate the analysis of the outer and inner flow is made in a new coordinate system. In order to fully understand the significance of this choice, it is necessary to make a regression to explain how a general change of coordinates is made. Switching from $x-y$ orthogonal coordinate system to an another generic orthogonal coordinate system $\Phi-\Psi$, the following relation is valid

$$\mathrm{d}x^2+\mathrm{d}y^2=h_\Phi^2\mathrm{d}\Phi^2+h_\Psi^2\mathrm{d}\Psi^2,$$

where h_Φ and h_Ψ are the transformation coefficients.
It can be easily demonstrated that

$$h_\Psi^2=\frac{(\frac{\partial\Phi}{\partial y})^2-(\frac{\partial\Phi}{\partial x})^2}{(\frac{\partial\Psi}{\partial x})^2(\frac{\partial\Phi}{\partial y})^2-(\frac{\partial\Phi}{\partial x})^2(\frac{\partial\Psi}{\partial y})^2}, \tag{A.1a}$$

$$h_\Phi^2=\frac{(\frac{\partial\Psi}{\partial x})^2-(\frac{\partial\Psi}{\partial y})^2}{(\frac{\partial\Psi}{\partial x})^2(\frac{\partial\Phi}{\partial y})^2-(\frac{\partial\Phi}{\partial x})^2(\frac{\partial\Psi}{\partial y})^2}. \tag{A.1b}$$

Now the general transformation coefficients can be calculated. A special orthogonal coordinate system is chosen, Φ-Ψ where Φ is the potential function and Ψ is the stream function of the outer mean flow $\widetilde{U}$ of components $\widetilde{U}$ and $\widetilde{V}$. By definition the following relations are valid:

$$\widetilde{U}=\frac{\partial\Phi}{\partial x}=\frac{\partial\Psi}{\partial y}; \tag{A.2a}$$

$$\widetilde{V}=\frac{\partial\Phi}{\partial y}=-\frac{\partial\Psi}{\partial x}. \tag{A.2b}$$

By calculating the transformation coefficient from (A.1a) and (A.1b) the result is that

$$h_\Phi^2=h_\Psi^2=\frac{1}{|\widetilde{\mathbf{U}}|^2}=\frac{1}{\widetilde{U}^2+\widetilde{V}^2}.$$

Then

$$\mathrm{d}x^2+\mathrm{d}y^2=h_\Phi^2\mathrm{d}\Phi^2+h_\Psi^2\mathrm{d}\Psi^2=\frac{\mathrm{d}\Phi^2+\mathrm{d}\Psi^2}{|\widetilde{\mathbf{U}}|^2}. \tag{A.3}$$

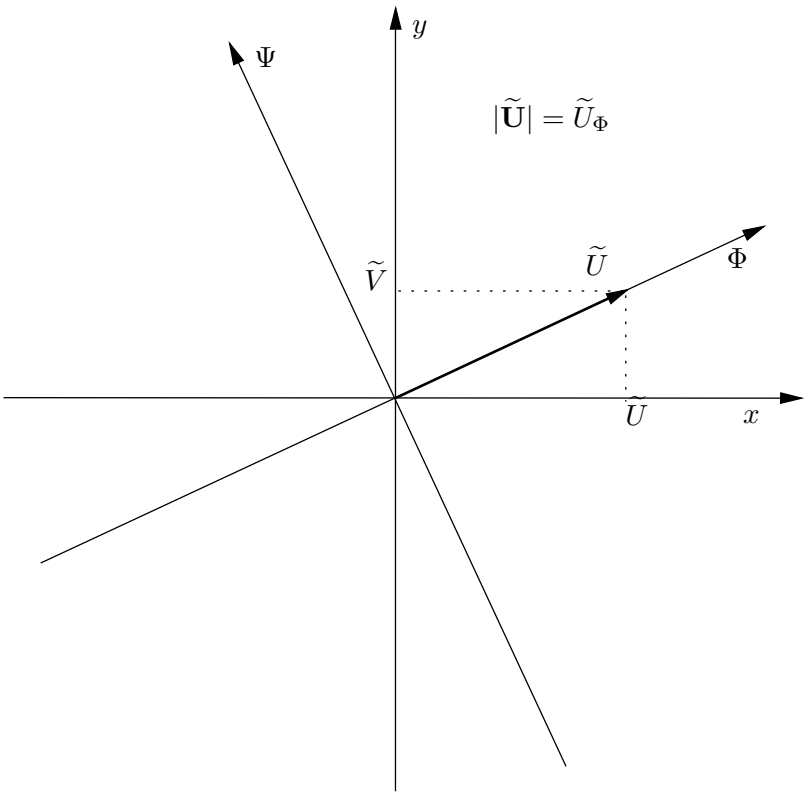

Fig. A.1: Outer potential velocity in x-y plane and Φ-Ψ plane.

The velocity $\widetilde{\mathbf{U}}$ is a vector in the Φ direction, because by definition a potential flow is along constant streamlines. Thus it has two components in the x-y plane, but just one component in the Φ-Ψ plane along Φ. This means that the absolute value of the velocity is the same value as the Φ-component, namely

$$|\widetilde{\mathbf{U}}| = \widetilde{U}_\Phi.$$

Figure A.1 shows the just explained relationship, which will be used when the coordinates of the equations will be changed.

The reason why it is convenient to change coordinates and in particular to choose the potential and stream function as new coordinates is that in this new system the body can be treated as a flat plate, because the stream lines follow the shape of the body as shown in Figure A.2.

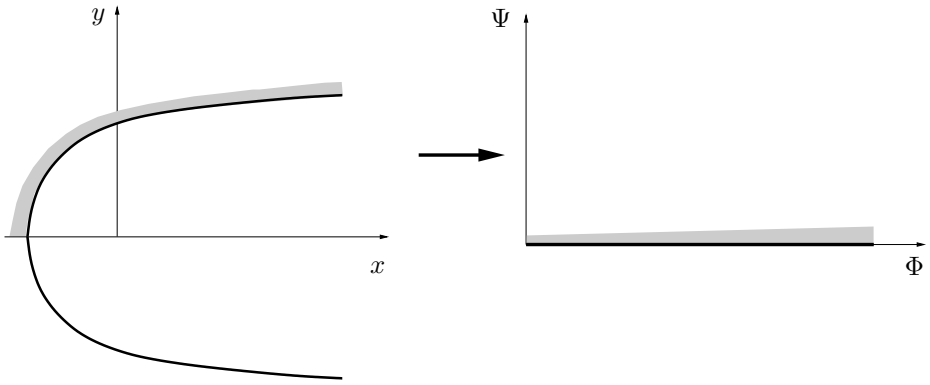

Fig. A.2: Change of coordinates.

Now it is important to see how gradient, divergence and curl operations change when the coordinate system changes. The function a is a scalar and A is a vector with components (A_Φ, A_Ψ, A_z) (these components are in the new directions); The new coordinate system is Φ, Ψ, z, the new directions are $\hat{e}_\Phi, \hat{e}_\Psi, \hat{e}_z$ and the transformation coefficients are h_Φ, h_Ψ, h_z. Then the following relations are valid:

$$\nabla \cdot \mathbf{A} = \frac{\partial A_x}{\partial x} + \frac{\partial A_y}{\partial y} + \frac{\partial A_z}{\partial z} = \frac{1}{h_\Phi h_\Psi h_z}\left[\frac{\partial(h_\Psi h_z A_\Phi)}{\partial \Phi} + \frac{\partial(h_\Phi h_z A_\Psi)}{\partial \Psi} + \frac{\partial(h_\Phi h_\Psi A_z)}{\partial z}\right], \tag{A.4a}$$

$$\nabla a = \hat{i}\frac{\partial a}{\partial x} + \hat{j}\frac{\partial a}{\partial y} + \hat{k}\frac{\partial a}{\partial z} = \hat{e}_\Phi \frac{1}{h_\Phi}\frac{\partial a}{\partial \Phi} + \hat{e}_\Psi \frac{1}{h_\Psi}\frac{\partial a}{\partial \Psi} + \hat{e}_z \frac{1}{h_z}\frac{\partial a}{\partial z}, \tag{A.4b}$$

$$\nabla \times \mathbf{A} = \hat{i}\left(\frac{\partial A_z}{\partial y} - \frac{\partial A_y}{\partial z}\right) - \hat{j}\left(\frac{\partial A_z}{\partial x} - \frac{\partial A_x}{\partial z}\right) + \hat{k}\left(\frac{\partial A_y}{\partial x} - \frac{\partial A_x}{\partial y}\right) = \tag{A.4c}$$

$$= \frac{1}{h_\Phi h_\Psi h_z}\left[\hat{e}_\Phi h_\Phi\left(\frac{\partial(h_z A_z)}{\partial \Psi} - \frac{\partial(h_\Psi A_\Psi)}{\partial z}\right) - \hat{e}_\Psi h_\Psi\left(\frac{\partial(h_z A_z)}{\partial \Phi} - \frac{\partial(h_\Phi A_\Phi)}{\partial z}\right) + \hat{e}_z h_z\left(\frac{\partial(h_\Psi A_\Psi)}{\partial \Phi} - \frac{\partial(h_\Phi A_\Phi)}{\partial \Psi}\right)\right].$$

Relations (A.4) are used to obtain continuity and Navier-Stokes equations in the new coordinate system. In the case considered here

$$h_\Phi = h_\Psi = \frac{1}{|\widetilde{\mathbf{U}}|},$$

$$h_z = 1.$$

In order to derive continuity and Navier-Stokes equations in optimal coordinates namely from (*x*,*y*,*z*) to (Φ,Ψ,*z*), the following equation is used to write the term $\nabla\cdot(\nabla\mathbf{V})$ in another way:

$$\nabla \cdot \nabla\mathbf{V} = \nabla(\nabla \cdot \mathbf{V}) - \nabla \times \nabla \times \mathbf{V}. \tag{A.5}$$

By the continuity equation the term $\nabla \cdot \mathbf{V}$ is zero. Thus (A.5) becomes

$$\nabla \cdot \nabla \mathbf{V} = -\nabla \times \nabla \times \mathbf{V}. \tag{A.6}$$

Moreover, it is easy to demonstrate the following relation:

$$\mathbf{V} \cdot \nabla \mathbf{V} = \nabla \left(\frac{|\mathbf{V}|^2}{2} \right) - \mathbf{V} \times \nabla \times \mathbf{V}. \tag{A.7}$$

By substituting (A.6) and (A.7) in the continuity and the following Navier-Stokes equations

$$\nabla \cdot \mathbf{V} = 0, \tag{A.8}$$

$$\frac{\partial \mathbf{V}}{\partial t} + \mathbf{V} \cdot \nabla \mathbf{V} = -\nabla p + \frac{1}{R} \nabla \cdot (\nabla \mathbf{V}), \tag{A.9}$$

where R is Reynolds number, it is obtained

$$\frac{\partial \mathbf{V}}{\partial t} + \nabla \left(\frac{|\mathbf{V}|^2}{2} \right) - \mathbf{V} \times \nabla \times \mathbf{V} = -\nabla p - \frac{1}{R} \nabla \times \nabla \times \mathbf{V}, \tag{A.10}$$

which is another form of the Navier-Stokes equation.

By equations (A.4) it is easy to see the the continuity equation in optimal coordinates is

$$\widetilde{U} \frac{\partial w_\Phi}{\partial \Phi} + \widetilde{U} \frac{\partial w_\Psi}{\partial \Psi} + \frac{\partial w_z}{\partial z} = 0, \tag{A.11}$$

where $\widetilde{U} = |\widetilde{\mathbf{U}}|$, $w_\Phi = u_\Phi / \widetilde{U}$, $w_\Psi = u_\Psi / \widetilde{U}$ and $w_z = w / \widetilde{U}$, with u_Φ and u_Ψ the velocity components in the Φ and Ψ directions respectively.

In order to find the Navier-Stokes equations in optimal coordinates the following passages are made:

$$\nabla \left(\frac{\mathbf{V}^2}{2} \right) = \begin{pmatrix} \widetilde{U} \frac{\partial}{\partial \Phi} \left(\frac{u^2+v^2+w^2}{2} \right) \\ \widetilde{U} \frac{\partial}{\partial \Psi} \left(\frac{u^2+v^2+w^2}{2} \right) \\ \frac{\partial}{\partial z} \left(\frac{u^2+v^2+w^2}{2} \right) \end{pmatrix}$$

$$\mathbf{V} \times \nabla \times \mathbf{V} = \widetilde{U}^2 \det \begin{pmatrix} 1 & 1 & 1 \\ u & v & w \\ \frac{1}{\widetilde{U}} \left[\frac{\partial w}{\partial \Psi} - \frac{\partial}{\partial z} \left(\frac{v}{\widetilde{U}} \right) \right] & \frac{1}{\widetilde{U}} \left[\frac{\partial}{\partial z} \left(\frac{u}{\widetilde{U}} \right) - \frac{\partial w}{\partial \Phi} \right] & \left[\frac{\partial}{\partial \Phi} \left(\frac{v}{\widetilde{U}} \right) - \frac{\partial}{\partial \Psi} \left(\frac{u}{\widetilde{U}} \right) \right] \end{pmatrix} =$$

$$= \widetilde{U}^2 \begin{pmatrix} v\left[\frac{\partial}{\partial\Phi}\left(\frac{v}{\widetilde{U}}\right) - \frac{\partial}{\partial\Psi}\left(\frac{u}{\widetilde{U}}\right)\right] - \frac{w}{\widetilde{U}}\left[\frac{\partial}{\partial z}\left(\frac{u}{\widetilde{U}}\right) - \frac{\partial w}{\partial\Phi}\right] \\ \frac{w}{\widetilde{U}}\left[\frac{\partial w}{\partial\Psi} - \frac{\partial}{\partial z}\left(\frac{v}{\widetilde{U}}\right)\right] - u\left[\frac{\partial}{\partial\Phi}\left(\frac{v}{\widetilde{U}}\right) - \frac{\partial}{\partial\Psi}\left(\frac{u}{\widetilde{U}}\right)\right] \\ \frac{u}{\widetilde{U}}\left[\frac{\partial}{\partial z}\left(\frac{u}{\widetilde{U}}\right) - \frac{\partial w}{\partial\Phi}\right] - \frac{v}{\widetilde{U}}\left[\frac{\partial w}{\partial\Psi} - \frac{\partial}{\partial z}\left(\frac{v}{\widetilde{U}}\right)\right] \end{pmatrix}$$

$$\nabla\times\nabla\times\mathbf{V} = \widetilde{U}^2 \det \begin{pmatrix} \frac{1}{\widetilde{U}}\left\{\frac{\partial}{\partial\Psi}\left\{\widetilde{U}^2\left[\frac{\partial}{\partial\Phi}\left(\frac{v}{\widetilde{U}}\right) - \frac{\partial}{\partial\Psi}\left(\frac{u}{\widetilde{U}}\right)\right]\right\} - \frac{\partial}{\partial z}\left[\frac{\partial}{\partial z}\left(\frac{u}{\widetilde{U}}\right) - \frac{\partial w}{\partial\Phi}\right]\right\} \\ \frac{1}{\widetilde{U}}\left\{\frac{\partial}{\partial z}\left[\frac{\partial w}{\partial\Psi} - \frac{\partial}{\partial z}\left(\frac{v}{\widetilde{U}}\right)\right] - \frac{\partial}{\partial\Phi}\left\{\widetilde{U}^2\left[\frac{\partial}{\partial\Phi}\left(\frac{v}{\widetilde{U}}\right) - \frac{\partial}{\partial\Psi}\left(\frac{u}{\widetilde{U}}\right)\right]\right\}\right\} \\ \frac{\partial}{\partial\Phi}\left[\frac{\partial}{\partial z}\left(\frac{u}{\widetilde{U}}\right) - \frac{\partial w}{\partial\Phi}\right] - \frac{\partial}{\partial\Psi}\left[\frac{\partial w}{\partial\Psi} - \frac{\partial}{\partial z}\left(\frac{v}{\widetilde{U}}\right)\right] \end{pmatrix}$$

and thus equation (A.10) in scalar form is

$$\Phi): \frac{\partial u}{\partial t} + \widetilde{U}\frac{\partial}{\partial\Phi}\left(\frac{u^2+v^2+w^2}{2}\right) - \widetilde{U}^2\left\{v\left[\frac{\partial}{\partial\Phi}\left(\frac{v}{\widetilde{U}}\right) - \frac{\partial}{\partial\Psi}\left(\frac{u}{\widetilde{U}}\right)\right] - \frac{w}{\widetilde{U}}\left[\frac{\partial}{\partial z}\left(\frac{u}{\widetilde{U}}\right) - \frac{\partial w}{\partial\Phi}\right]\right\} =$$

$$-\widetilde{U}\frac{\partial p}{\partial\Phi} - \frac{\widetilde{U}}{R}\left\{\frac{\partial}{\partial\Psi}\left\{\widetilde{U}^2\left[\frac{\partial}{\partial\Phi}\left(\frac{v}{\widetilde{U}}\right) - \frac{\partial}{\partial\Psi}\left(\frac{u}{\widetilde{U}}\right)\right]\right\} - \frac{\partial}{\partial z}\left[\frac{\partial}{\partial z}\left(\frac{u}{\widetilde{U}}\right) - \frac{\partial w}{\partial\Phi}\right]\right\}$$

$$\Psi): \frac{\partial v}{\partial t} + \widetilde{U}\frac{\partial}{\partial\Psi}\left(\frac{u^2+v^2+w^2}{2}\right) - \widetilde{U}^2\left\{\frac{w}{\widetilde{U}}\left[\frac{\partial w}{\partial\Psi} - \frac{\partial}{\partial z}\left(\frac{v}{\widetilde{U}}\right)\right] - u\left[\frac{\partial}{\partial\Phi}\left(\frac{v}{\widetilde{U}}\right) - \frac{\partial}{\partial\Psi}\left(\frac{u}{\widetilde{U}}\right)\right]\right\} =$$

$$-\widetilde{U}\frac{\partial p}{\partial\Psi} - \frac{\widetilde{U}}{R}\left\{\frac{\partial}{\partial z}\left[\frac{\partial w}{\partial\Psi} - \frac{\partial}{\partial z}\left(\frac{v}{\widetilde{U}}\right)\right] - \frac{\partial}{\partial\Phi}\left\{\widetilde{U}^2\left[\frac{\partial}{\partial\Phi}\left(\frac{v}{\widetilde{U}}\right) - \frac{\partial}{\partial\Psi}\left(\frac{u}{\widetilde{U}}\right)\right]\right\}\right\}$$

$$z): \frac{\partial w}{\partial t} + \frac{\partial}{\partial z}\left(\frac{u^2+v^2+w^2}{2}\right) - \widetilde{U}\left\{u\left[\frac{\partial}{\partial z}\left(\frac{u}{\widetilde{U}}\right) - \frac{\partial w}{\partial\Phi}\right] - v\left[\frac{\partial w}{\partial\Psi} - \frac{\partial}{\partial z}\left(\frac{v}{\widetilde{U}}\right)\right]\right\} =$$

$$-\frac{\partial p}{\partial z} - \frac{\widetilde{U}^2}{R}\left\{\frac{\partial}{\partial\Phi}\left[\frac{\partial}{\partial z}\left(\frac{u}{\widetilde{U}}\right) - \frac{\partial w}{\partial\Phi}\right] - \frac{\partial}{\partial\Psi}\left[\frac{\partial w}{\partial\Psi} - \frac{\partial}{\partial z}\left(\frac{v}{\widetilde{U}}\right)\right]\right\}$$

where u,v,w are the velocity components in the Φ,Ψ,z directions (not in x,y,z directions). Rearranging and simplifying it is obtained

$$\Phi): \frac{1}{\widetilde{U}^2}\frac{\partial w_\Phi}{\partial t} + w_\Phi\frac{\partial w_\Phi}{\partial \Phi} + w_\Psi\frac{\partial w_\Phi}{\partial \Psi} + \frac{w_z}{\widetilde{U}}\frac{\partial w_\Phi}{\partial z} + (w_\Phi^2 + w_\Psi^2)\frac{\partial}{\partial \Phi}(\ln \widetilde{U}) =$$
$$-\frac{1}{V_0^2}\frac{\partial p}{\partial \Phi} + \frac{1}{R}\left[\frac{\partial^2 w_\Phi}{\partial \Phi^2} + \frac{\partial^2 w_\Phi}{\partial \Psi^2} + \frac{1}{V_0^2}\frac{\partial^2 w_\Phi}{\partial z^2} - 2\frac{\partial \ln \widetilde{U}}{\partial \Psi}\left(\frac{\partial w_\Psi}{\partial \Phi} - \frac{\partial w_\Phi}{\partial \Psi}\right) - \frac{2}{\widetilde{U}}\frac{\partial \ln \widetilde{U}}{\partial \Phi}\frac{\partial w_z}{\partial z}\right]$$

$$\Psi): \frac{1}{\widetilde{U}^2}\frac{\partial w_\Psi}{\partial t} + w_\Phi\frac{\partial w_\Psi}{\partial \Phi} + w_\Psi\frac{\partial w_\Psi}{\partial \Psi} + \frac{w_z}{\widetilde{U}}\frac{\partial w_\Psi}{\partial z} + (w_\Phi^2 + w_\Psi^2)\frac{\partial}{\partial \Psi}(\ln \widetilde{U}) =$$
$$-\frac{1}{V_0^2}\frac{\partial p}{\partial \Psi} + \frac{1}{R}\left[\frac{\partial^2 w_\Psi}{\partial \Phi^2} + \frac{\partial^2 w_\Psi}{\partial \Psi^2} + \frac{1}{V_0^2}\frac{\partial^2 w_\Psi}{\partial z^2} + 2\frac{\partial \ln \widetilde{U}}{\partial \Phi}\left(\frac{\partial w_\Psi}{\partial \Phi} - \frac{\partial w_\Phi}{\partial \Psi}\right) - \frac{2}{\widetilde{U}}\frac{\partial \ln \widetilde{U}}{\partial \Psi}\frac{\partial w_z}{\partial z}\right]$$

$$z): \frac{1}{\widetilde{U}^2}\frac{\partial w_z}{\partial t} + w_\Phi\frac{\partial w_z}{\partial \Phi} + w_\Psi\frac{\partial w_z}{\partial \Psi} + \frac{w_z}{\widetilde{U}}\frac{\partial w_z}{\partial z} + w_z\left(w_\Phi\frac{\partial \ln \widetilde{U}}{\partial \Phi} + w_\Psi\frac{\partial \ln \widetilde{U}}{\partial \Psi}\right) =$$
$$-\frac{1}{V_0^3}\frac{\partial p}{\partial z} + \frac{1}{R}\left[\frac{\partial^2 w_z}{\partial \Phi^2} + \frac{\partial^2 w_z}{\partial \Psi^2} + \frac{1}{V_0^2}\frac{\partial^2 w_z}{\partial z^2} + \frac{w_z}{\widetilde{U}}\left(\frac{\partial^2 \widetilde{U}}{\partial \Phi^2} + \frac{\partial^2 \widetilde{U}}{\partial \Psi^2}\right) + 2\left(\frac{\partial w_z}{\partial \Phi}\frac{\partial \ln \widetilde{U}}{\partial \Phi} + \frac{\partial w_z}{\partial \Psi}\frac{\partial \ln \widetilde{U}}{\partial \Psi}\right)\right]$$

B. NUMERICAL PROCEDURE FOR BOUNDARY LAYER EQUATIONS

In order to solve the boundary region equations a marching procedure along $\bar{\Phi}$ is used. The method is based on second-order central differences in η and backward differences in $\bar{\Phi}$. The grid used to compute the pressure is staggered compared to the grid used for the velocity components as shown in Figure B.1.

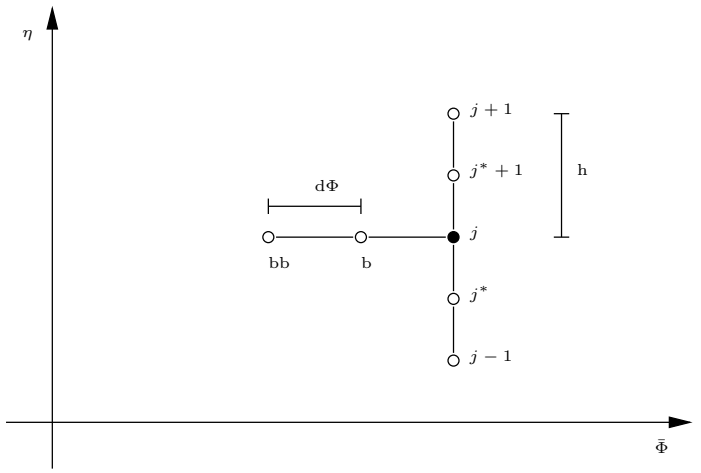

Fig. B.1: Grid used to compute the velocity components and pressure.

With the second-order central differences method a function f and its first and second derivatives are approximated as follows:

$$f = f_j, \tag{B.1}$$

$$\frac{\partial f}{\partial \eta} = \frac{f_{j+1} - f_{j-1}}{2h}, \tag{B.2}$$

$$\frac{\partial^2 f}{\partial \eta^2} = \frac{f_{j+1} - 2f_j + f_{j-1}}{h^2}. \tag{B.3}$$

With the second-order backward differences method the first derivative of a function f is given by:

$$\frac{\partial f}{\partial \bar{\Phi}} = \frac{a f_j + b f_{bj} + c f_{bbj}}{\mathrm{d}\Phi}, \tag{B.4}$$

where a, b and c are assigned values.

The grid of pressure is staggered, thus the value of the pressure in (3.69) and its derivative with respect to η in (3.68) have been expressed in terms of the staggered index, namely

$$\bar{p} = \frac{\bar{p}_{j^*+1} + \bar{p_{j^*}}}{2}, \tag{B.5}$$

$$\frac{\partial \bar{p}}{\partial \eta} = \frac{\bar{p}_{j^*+1} - \bar{p}_{j^*}}{h}, \tag{B.6}$$

as can be easily seen in Figure B.1.

The index j goes from 0 to $N-1$, thus the boundary conditions are:

$$\bar{u}_{j=0} = \bar{v}_{j=0} = \bar{w}_{j=0} = 0, \tag{B.7}$$

$$\bar{u}_{j=N-1} = 0, \tag{B.8}$$

$$\bar{v}_{j=N-1} = -i\frac{\tilde{v}(\bar{\Phi}, N-1)}{k\widetilde{U}_b(\bar{\Phi}, N-1)\sqrt{2\bar{\Phi}}}, \tag{B.9}$$

$$\bar{w}_{j=N-1} = \frac{\tilde{w}(\bar{\Phi}, N-1)}{\widetilde{U}_b(\Phi, N-1)}, \tag{B.10}$$

$$\bar{p}_{j=N-1} = \tilde{p}_0(\bar{\Phi}, N-1.) \tag{B.11}$$

The linearised parabolic system have a block tridiagonal structure which can be solved with Keller's Box method .This block elimination method consists of two sweeps, one *forward* and one *backward*. At each step j the unknown functions are computed from recursion formulas.

BIBLIOGRAPHY

Anderson, J.D. Jr. 2007. *Fundamentals of aerodynamics*. 4 edn. McGraw Hill.

Bender, M., & Orszag, S. A. 1999. *Advanced Mathematical Methods for Scientists and Engineers - Asymptotic methods and perturbation theory*. Springer.

Cebeci, T. 2002. *Convective Heat Transfer*. Springer-Verlag.

Goldstein, M.E. 1978. Unsteady vortical and entropic distortions of potential flows round arbitrary obstacles. *J. Fluid Mech.*, **89**, 433–468.

Goldstein, M.E. 1984. Small-amplitude viscous motion on arbitrary potential flows. *Quart. J. Mech. Appl. Math.*, **37**, 1–31.

Holmes, M. H. 2013. *Introduction to Perturbation Methods*. Springer.

Hunt, J.C.R. 1973. A theory of turbulent flow round two-dimensional bluff bodies. *J. Fluid Mech.*, **61**(04), 625–706.

Jacobs, R.G., & Durbin, P.A. 2001. Simulation of bypass transition. *J. Fluid Mech.*, **428**, 185–212.

Kendall, J.M. 1990. Boundary layer receptivity to free stream turbulence. *AIAA Paper*, **90-1504**.

Ladyzhenskaya, O.A., & Silverman, R.A. 1969. *The mathematical theory of viscous incompressible flow*. Gordon and Breach.

Leib, S.J., Wundrow, D.W., & Goldstein, M.E. 1999a. Effect of free-stream turbulence and other vortical disturbances on a laminar boundary layer. *J. Fluid Mech.*, **380**, 169–203.

Leib, S.J., Wundrow, D.W., & Goldstein, M.E. 1999b. Generation and growth of boundary-layer disturbances due to free-stream turbulence. *AIAA Paper 99-0498*.

Luchini, P. 2000. Reynolds-number-independent instability of the boundary layer over a flat surface: optimal perturbations. *J. Fluid Mech.*, **404**, 289–309.

Matsubara, M., & Alfredsson, P.H. 2001. Disturbance growth in boundary layers subjected to free-stream turbulence. *J. Fluid Mech.*, **430**, 149–168.

Panton, R. 1995. *Incompressible Flow*. Wiley-Interscience – Second Edition.

Ricco, P., Luo, J., & Wu, X. 2011. Evolution and instability of unsteady nonlinear streaks generated by free-stream vortical disturbances. *J. Fluid Mech.*, **677**, 1–38.

Schlichting, H. 1979. *Boundary-layer theory.* McGraw Hill.Inc.

Wundrow, D.W., & Goldstein, M.E. 2001. Effect on a laminar boundary layer of small-amplitude streamwise vorticity in the upstream flow. *J. Fluid Mech.*, **426**, 229–262.

Zaki, T., & Durbin, P.A. 2005. Mode interaction and the bypass route to transition. *J. Fluid Mech.*, **531**, 85–111.

ACKNOWLEDGEMENTS

We would like to thank Air Force Of Scientific Research (AFOSR) (Grant FA8655-13-1-3073 DEF) for funding this work, with particular regards to Dr. Gregg Abate and Dr. Russ Cummings. We also acknowledge the interesting discussions with Dr. M. E. Goldstein and Dr. S. J. Leib at Glenn Research Center (Cleveland, OH). This work was presented at the Annual Contractor Review for the Aerothermodynamics program at AFOSR, Arlington (VA), held at the AFOSR BRICC (Basic Research Innovation Collaboration Center), in June 2016.